

Investigations of pond metabolism in temperate salt marshes of Massachusetts

Author: Gyujong Yoo

Persistent link: <http://hdl.handle.net/2345/bc-ir:108062>

This work is posted on [eScholarship@BC](#),
Boston College University Libraries.

Boston College Electronic Thesis or Dissertation, 2018

Copyright is held by the author, with all rights reserved, unless otherwise noted.

Abstract

Salt marshes provide important ecosystem services, including carbon sequestration. Permanently inundated ponds are prominent features in the marsh landscape, encompassing up to 60% of the total marsh area, but they are rarely considered in biogeochemical assessments. I investigated two ponds in Plum Island Estuary, MA to measure and analyze their metabolism. The ponds varied in size and vegetation cover. Oxygen concentrations and pH values were recorded in 15-minute intervals during the entire study period. The ponds regularly become hypoxic or anoxic during night. This is a problem for the estimation of respiration rates which are based on nighttime measurements. To investigate this potential underestimation, several approaches to estimate respiration were used. First, additional measurements of surface water concentrations of dissolved inorganic carbon were made. A comparison of respiration estimates based on oxygen and DIC changes during tidal isolation revealed a reasonable agreement for the most time but not during periods of high productivity during the day or late at night. At this point, oxygen concentrations are so depleted that a change in concentration – the indicator of respiration – is barely detectable. However, DIC based respiration rates indicate that respiration is occurring under these hypoxic/anoxic conditions. This saturation changes during periods of tidal inundation, when a nighttime peak in oxygen concentrations indicates that the flood water is relatively enriched in oxygen compared to the pond water. On three days, it was tested whether under these conditions the oxygen-based respiration rate was higher than under hypoxic conditions (i.e., during tidal isolation). The rates were indeed higher than those under tidal isolation but still not in the range of DIC-based rates. Overall, metabolic rates differed between the two ponds in magnitude, which is likely caused by different vegetation cover, but may be influenced by size, sampling period, and duration as well.

BOSTON COLLEGE DEPARTMENT OF EARTH AND ENVIRONMENTAL SCIENCES

Investigations of Pond Metabolism in Temperate Salt Marshes of Massachusetts

Senior Thesis

Department of Earth and Environmental Sciences

Gyujong Yoo

2018 April 20

Contents

Introduction.....	3
Methods.....	10
Research Site.....	10
Oxygen Measurements.....	16
Determination of Tidal Flushing.....	16
DIC Measurements	17
Metabolic Rates	21
Results	25
Pond 1	25
Environmental Conditions	25
Periods of Tidal Flushing.....	26
Oxygen Concentrations.....	30
DIC Concentrations	32
Metabolism – Oxygen.....	35
Metabolism – DIC.....	35
Comparison of Rates – Oxygen and DIC	37
Pond 2	40
Discussion	42
Estimation of Respiration in Salt Marsh Ponds	42
Ponds as Part of the Landscape.....	45
Summary.....	48
Acknowledgements	50

1. Introduction

Salt marshes are coastal environments that provide a range of valuable ecosystem services. They play an integral role in the aquatic food web through providing a linkage between freshwater rivers and streams to the oceans. Salt marshes allow for a delivery of nutrients and sediment to coastal waters, as well as providing coastal protection (Woodroffe, 2002). They support a myriad of terrestrial and aquatic species. Many animals seek refuge in salt marshes, especially many marine fish that use salt marshes as nursing grounds for juveniles. Salt marshes have the highest rates of organic matter (OM) production and storage per acre in comparison to other coastal environments (Barbier et al., 2010; McLeod et al., 2011). The capability of carbon sequestration is becoming increasingly pertinent as anthropogenic and natural disturbances reduce the productivity of the marsh vegetation and the drainage of marsh soils, and as salt marshes are threatened by sea level rise and land use change (Milette et al., 2010; Hopkinson et al., 2012).

Salt marshes occur on low-energy shorelines resulting from dissipation of storm waves passing over initial dunes, and they occur usually in temperate climates and high-latitudes (Allen and Pye, 1992). Most salt marshes are characterized by low topography but a vast expanse of area. The shorelines of marshes are commonly areas formed by deposition of sediments from streams called tidal flats, and these areas are nourished with silt, clay, and detritus from inflowing rivers and streams (Chapman, 1974). Salt marshes occur essentially worldwide; they were mapped in 99 countries by Mcowen et al. (2017).

The formation of salt marshes begins with the accretion of sediments onto the tidal flats. As the tidal flats gain elevation relative to the sea level, vegetation can colonize the exposed

surface due to the decrease of the rate and duration of tidal inundation (Bird, 2008; Pethick, 1984). As waters from rivers and streams arrive at salt marshes, the discharge rate decreases and suspended sediment settles (Chapman, 1974). The establishment of vegetation and other photosynthesizing organisms (i.e., algae) allow for increased erosion resistance and sediment settlement. This, in tangent with the continual deposition on salt marsh terraces, allows for competition amongst species and in often times developments of successive plant communities (Pethick, 1984).

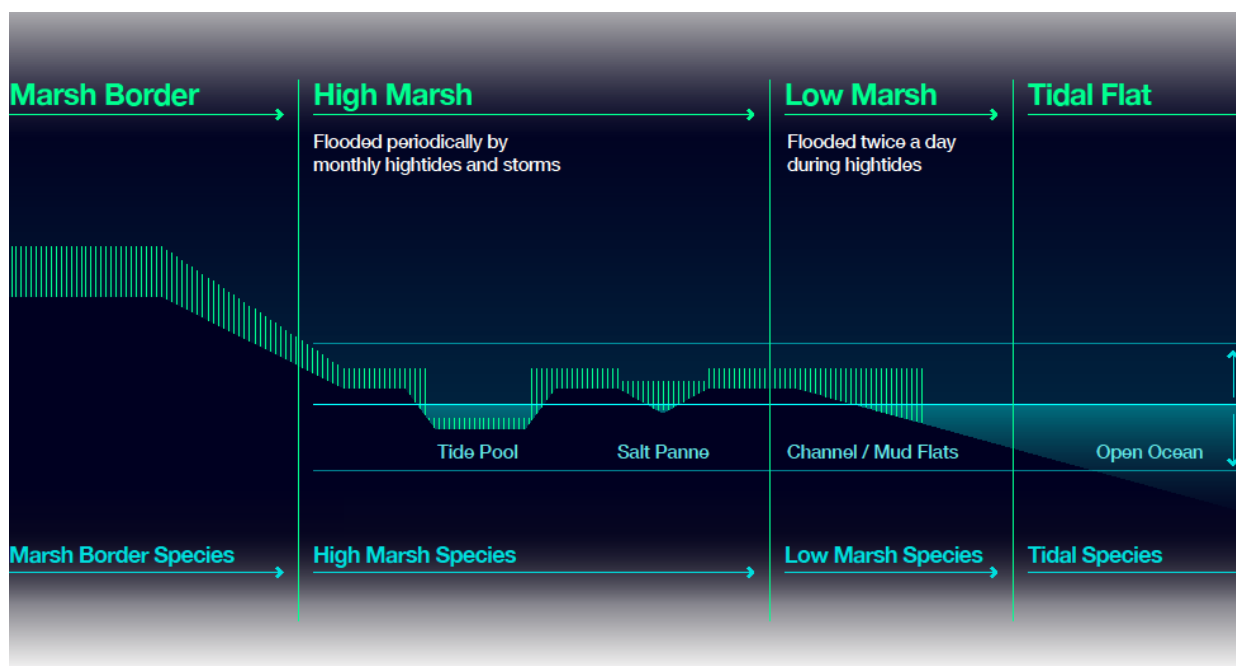


Figure 1. A diagram displaying the distinctions of the high marsh and low marsh in regards to susceptibility of flooding. Ocean Health Index (2018).

The salt marsh landscape includes areas of high and low elevation, each populated with different species of emergent grasses and dense stands of salt-tolerant bushes, shrubs, and herbs (Adam, 1990). There are two distinct zones within the landscape: high marsh and low marsh

(Figure 1). The shape and appearance of these zones result from unique, complex interactions of local topography and bathymetry, sea level rise, tidal inundation, sediment supply and vegetation (Nixon, 1982). The high marsh, in contrast to the low marsh, is characterized by the infrequent inundation during periods of extremely high tide conditions (i.e., spring tide) and storm surges associated with coastal storms. High marshes are also contrasted with low marshes in regards to plant and animal communities; high marshes are dominated by marsh hay *Spartina patens* and *S. alterniflora* (short form), while low marshes are dominated by the smooth cordgrass *Spartina alterniflora* (tall form) [Bertness, 1991].

In many locations, particularly in the northeastern United States, the landscape is incised by man-made channels, and it is also dotted with relatively small ponds. Salt marsh ponds form through physical and biogeochemical processes (Miller and Egler, 1950). Permanently inundated ponds occupy from 1-60% of salt marsh platforms (Adamowicz and Roman, 2005; Milette et al., 2010). The ponds are relatively shallow – usually 20-30 cm – and have varying surface areas, ranging from a couple square meters to greater than several thousands of meters (Spivak et al., 2017). However, they are rarely characterized and factored into whole-ecosystem assessments (Spivak et al., 2018).

The primary catalyst of pond formation is the waterlogging of marsh soils due to increased tidal inundation and reduced drainage efficiency, which leads to the dieback of emergent vegetation (Burdick and Mendelsohn, 1990; Mendelsohn and McKee, 1988). Other mechanisms can also lead to the dieback of vegetation, including intense grazing by primary consumers and deposition of macroalgal and macrophyte wrack (Tolley and Christian, 1999). The patches of denuded soil are then subject to depression and expansion through a combination

of processes including erosion, slumping, compaction, and decomposition of peat (Ganju et al., 2015; Mariotti and Fagherazzi, 2013; Spivak et al., 2017; van Huissteden and van de Plassche, 1998).

Salt marsh ponds do not receive a regular supply of sediment with inundation, and the resulting hypersaline and anoxic conditions of the standing water inhibit marsh grass production (Johnston et al., 2003). The formation of stagnant ponds in salt marshes may reduce OM storage in soils, grass productivity and OM trapping, and changes in microbial community metabolisms (Spivak et al., 2017). Ponds may either represent a permanent loss of vegetated marsh habitat or undergo cycles of formation, drainage and revegetation (Schepers et al., 2017; Wilson et al., 2014). At Plum Island, it is still unclear if ponds have a cyclic behavior (i.e., they connect or disconnect to creeks and/or ditches, or if they are indeed permanent) (Wilson et al., 2014; Spivak et al., 2017). The combination of pond formation and loss of vegetation has the potential to affect carbon storage of salt marshes.

The biogeochemistry and ecology of ponds are likely affected by irregularities in tidal flushing. Ponds that are situated in the high marsh and only flushed during spring and storm tides are isolated from inputs of new saltwater for days to even weeks (Milette et al., 2010). During this period of isolation, evaporation and warming may concentrate salts and metabolites that, in turn, affect the rates of primary production and heterotrophic metabolisms (i.e., respiration). Tidal flushing can reset the chemistry of the surface water and bring OM from the ponds into tidal creeks and the marsh platform, similarly to the flooding events on floodplain ecosystems (Ahearn et al., 2006).

Measurements of whole system or ecosystem metabolism in aquatic systems are ideally done by continuous measurements of concentrations of dissolved oxygen and/or dissolved inorganic carbon (Staeher et al., 2010). Concentration changes occur during 24-hour periods that are associated with both respiration and photosynthesis during daylight and only respiration during the night. Salt marsh ponds become anoxic during the night (Spivak et al., 2017), and during these periods respiration rates based on oxygen will underestimate anaerobic respiration, because it will not affect oxygen concentrations. More accurate rates of respiration – and consequently gross primary production – cannot be estimated using only oxygen as a metric; one must account for anaerobic processes which are not represented by oxygen. Using a second metric, such as dissolved inorganic carbon (DIC) allows for a better representation of respiration in anaerobic systems such as salt marsh ponds.

The different species of DIC in the samples (i.e., carbon dioxide, bicarbonate, and carbonate) and their respective concentrations can be described by the Bjerrum plot (**Figure 2**). The Bjerrum plot graphs the concentrations of the different species as functions of a solution's pH in a logarithmic scale. Changes in pH do not affect the overall concentration of DIC but rather changes the distribution of its species. In acidic conditions, the dominant form is CO₂ (aqueous carbon dioxide). In basic conditions, the dominant form is CO₃²⁻ (carbonate ion). In between, the dominant form is HCO₃⁻ (bicarbonate ion). The various species interconvert readily dependent on pH, and compositional balance of DIC species as a function of pH can be visualized by the Bjerrum plot (**Figure 2**) [Glazer, 2013]. Changes to the concentration of one species lead to a redistribution of concentrations of other species.

$$DIC = [CO_{2(aq)}] + [H_2CO_3] + [HCO_3^-] + [CO_3^{2-}]$$

At pH of seawater, more than 99% of DIC species are HCO_3^- and CO_3^{2-} , which is why it was important to utilize DIC analyzers.

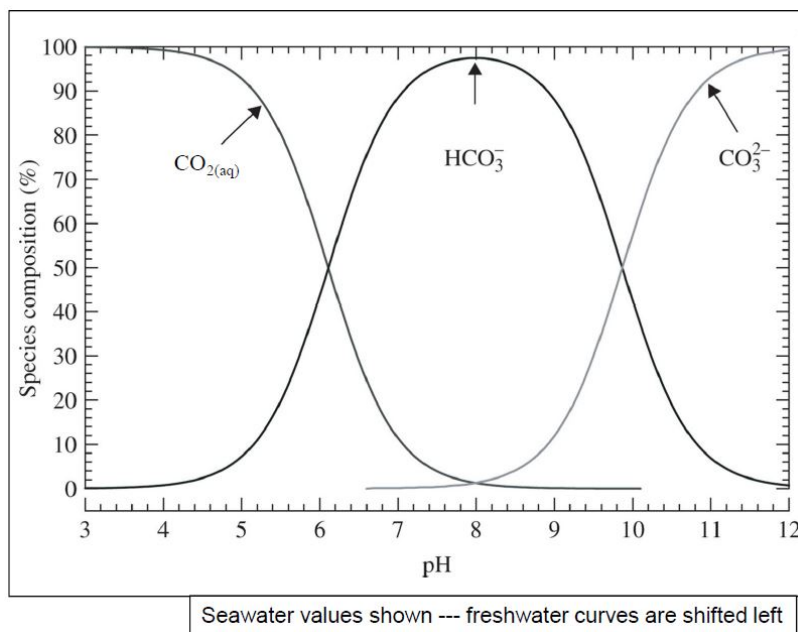


Figure 2. A Bjerrum plot, showing the species composition of DIC in seawater as a function of pH. Courtesy of Greenway et al. (2006). Note that at $\text{pH} < 4$, 100% of the total dissolved inorganic carbon is $\text{CO}_{2(\text{aq})}$, at $\text{pH} = 8$, bicarbonate is at maximum, and at $\text{pH} > 12$ carbonate is at maximum.

Historically, human actions have led to considerable loss and changes of salt marshes, and there are increasing encroachments onto limited, undisturbed ecosystems. The coast is a highly attractive natural feature to humans, through its aesthetics, resources, and availability. The low topography and vast area of salt marshes make it hugely popular for human populations (Bromberg-Gedan et al., 2009). As a result, 123.3 million people, or 39% of the United States' population, lived in counties directly on the shoreline, and the population is expected to increase by 8% from 2010 to 2020 (NOAA, 2010). The study of these environments is becoming increasingly important because of national and anthropogenic disturbances that can reduce the productivity of emergent vegetation and drainage properties of marsh soils. These perturbations, including sea level rise, erosion, and infilling of man-made mosquito ditches, can contribute to

an expansion of the number and size of shallow ponds that are scattered throughout the marsh landscape. It is rather ambiguous how the change in habitat composition will affect in the resulting functionality of the ecosystem. This is in part because while key biological processes are well characterized in high and low marsh habitats, these processes are less well understood in salt marsh ponds (Spivak et al., 2017).

There have been extensive examinations of salt marshes and their inhabitants under natural, experimental, and human-impacted settings for decades, which have led to a fundamental understanding of how marshes function and respond to disturbances. It is important to effectively characterize pond biogeochemistry and metabolism if we are to improve our current understanding of the ecosystem functioning of salt marshes. Developing a more comprehensive and holistic knowledge of marsh functionality can be helpful to our ability to predict future trends of pond formation. Estimating metabolism is an important aspect of increasing our understanding of salt marsh ponds, as metabolism is a foundational process embedded in ecosystems. It extends through multiple scales of organization, from the organismal scale to an entire ecosystem scale.

In this study, I quantified pond metabolic rates across tide stages of isolation and flushing. I investigated the frequency and the duration of tidal flushing of pond surface waters. After identifying the period of inundation, I analyzed the changes of concentrations in oxygen and dissolved inorganic carbon (DIC). These two concentrations would serve as different metrics in estimating rates of metabolic processes of gross primary production (GPP), net ecosystem production (NEP), and respiration (R): there would be a greater likelihood of nighttime hypoxia (or anoxia) during periods of tidal isolation than periods tidal flushing. I assess the impact this

has on respiration estimates by a) comparing rates based on oxygen and DIC and b) studying the effect tidal flushing has on oxygen changes at night. In addition, I examined the relationship between the abundance of vascular aquatic vegetation in the pond, in particular the widgeon grass *Ruppia maritima*, and rates of pond metabolism.

2. Methods

2.1 Research Site

This research took place at the Plum Island Ecosystems (PIE) Long Term Ecological Research (LTER) site located in northeastern Massachusetts (-71.22W, -70.75E, 42.89N, 42.5S; **Figure 3**) [MBL PIE-LTER, 2017]. PIE LTER is administered the by The Ecosystems Center, Marine Biological Laboratory, Woods Hole, MA. PIE is a member of the US Long Term Ecological Research Network funded by the National Science Foundation's Long Term Ecological Research Program. The salt marsh landscape experiences semi-diurnal tides, with a mean range of 2.9 m (Spivak et al., 2017). The emergent vegetation in the high marshes is dominated by *Spartina patens*, short-form *Spartina alterniflora*, and *Distichlis spicata* (~1.4 m above North American Vertical Datum of 1988 [NAVD88]) [Milette et al., 2010]. The high marsh platform is also incised by natural creeks as well as man-made tidal creeks and depression-era drainage ditches.

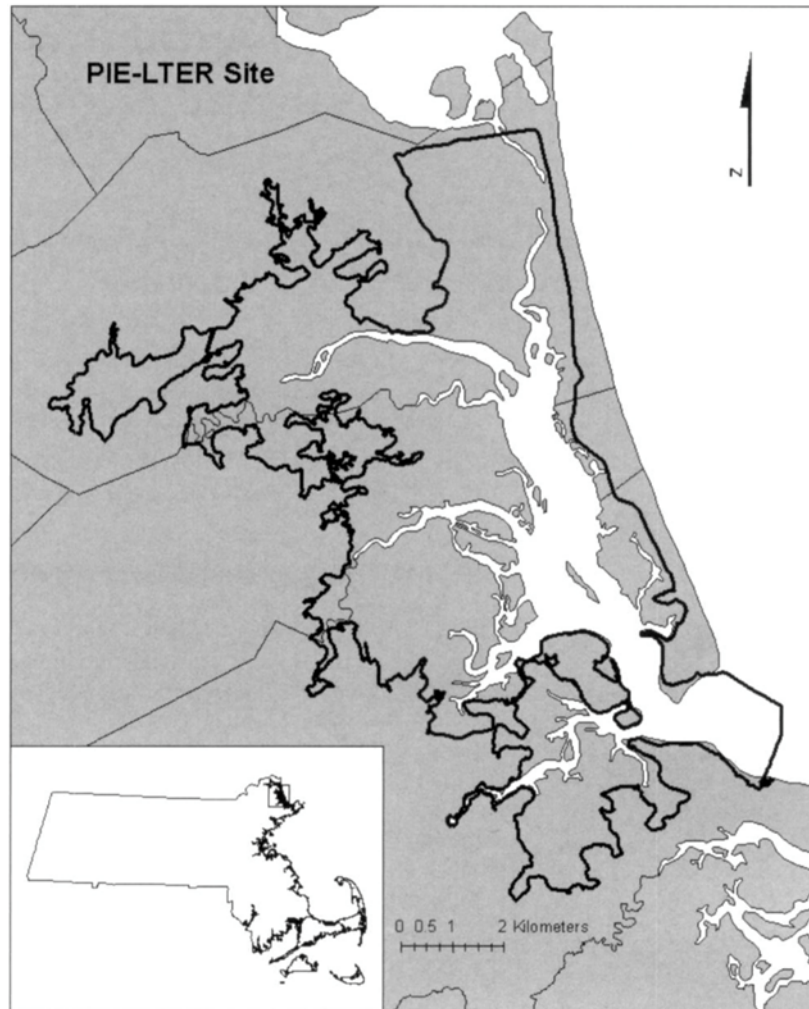


Figure 3. The Plum Island Estuary Long Term Ecological Research (PIE-LTER) study area, located in northeast Massachusetts. Map courtesy of Milette et al. (2010).

I chose two ponds that were permanently inundated with distinct perimeters, and thus were not connected to other ponds. The larger of the two ponds was named Pond 1, and the other Pond 2 (**Figure 4**). Ponds 1 and 2 were located at similar elevations in the high marsh (1.44 m above NAVD88) [**Figures 6, 7**]. The surface area in Pond 1 was 931 m². The surface area in Pond 2 was 26.34 m². The average depth of both ponds was 0.33 m. Ponds in the high marsh were chosen over the ponds in the low marsh as part of a larger study of pond metabolism, because they would be less frequently affected by tidal flooding. Their infrequent flooding

frequent allows separating for different flooding regimes. Due to physical limitations, ponds chosen for the study needed to be easily accessible by automobile and foot.

The two ponds varied in surface area, depth, and primary producer communities – particularly the presence of aquatic vegetation *R. maritima* (**Figure 5**). I took samples of the water column (~5 cm) throughout five sampling sessions, which took place between June 21 and July 28, 2017 for Pond 1 and between August 2 and August 3, 2017 for Pond 2. These five sampling events encompassed both periods of tidal isolation and tidal flushing. Four of the five sampling events were in Pond 1, and the fifth sampling event was in Pond 2. Session 1 took place from Jun 21 to June 22, Session 2 from June 28 to 29, Session 3 from July 5 to July 6, Session 4 from June 26 to 27, and Session 5 from August 2 to 3. There were 62 samples collected in Pond 1 (Sessions 1, 2, 3, and 4) and 8 samples collected in Pond 2 (Session 5). Due to limitations in equipment and time, the samples were not taken simultaneously at both sampling sites. Periods of tidal flushing were indicated by the overtopping of the marsh platform by high tides and the connection to water in the ponds.



Figure 4. Aerial imagery of a section of the high marsh of PIE-LTER. Pond 1 and Pond 2 are labeled. The distance between the two ponds is 42 meters. Aerial image courtesy of Google Earth.

The abundance of pond plant communities (i.e., macroalgae *Ulva* and *R. maritima*) was determined by visual estimation. The percent cover was estimated by visual inspection of six, 1 m² quadrats, randomly placed at three locations along each of the two transects across the pond. Atmospheric conditions were consistently recorded at 15-minute intervals by three meteorological towers on the marshes; wind speed (m s⁻¹) and temperature (°C) were measured 14 m above the marsh platform (Forbrich and Giblin, 2015).



Figure 5. Dominant vegetation of the high marshes of PIE-LTER. Clockwise from top left: *Spartina alterniflora* (short term), *Spartina patens*, *Ruppia maritima*, *Distichlis spicata*. *S. alterniflora*, *S. patens*, and *D. spicata* are emergent grasses of the marsh platform. *R. maritima* is a submerged grass found in numerous ponds. Images courtesy of Sandy richard, Dana Filipinni, Marilee Lovit, and Glen Mittelhauser, respectively.



Figure 6. Picture of Pond 1 in early July, 2017. Communities of *R. maritima* can be seen in green patches in the water. Communities of macroalgae *Ulva* are also seen in brown patches in the water.

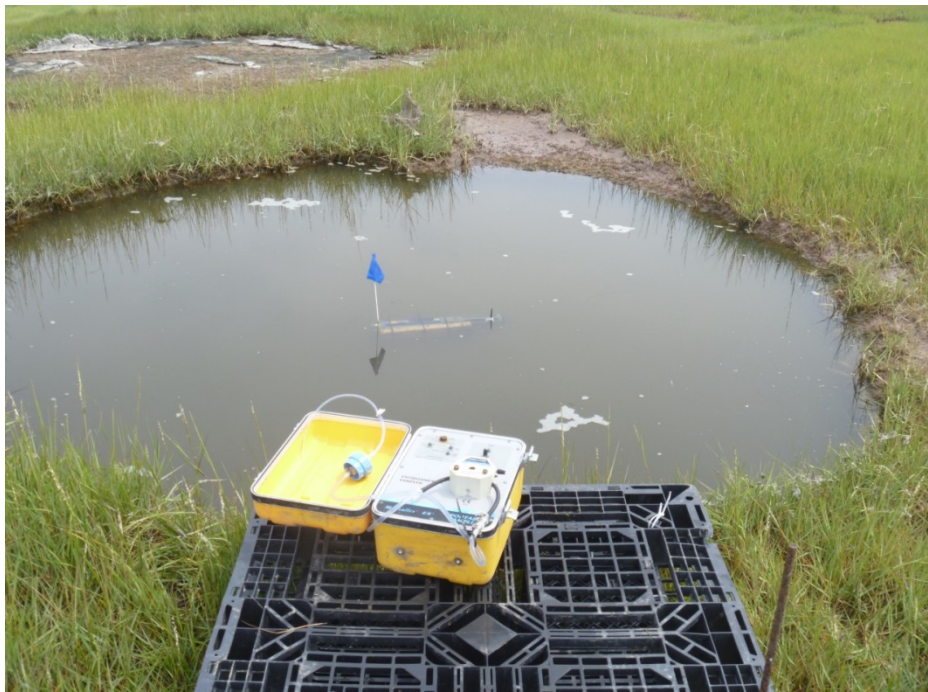


Figure 7. Picture of Pond 2 in early August, 2017. Communities of macroalgae were small in number (and not visible). Communities of *R. maritima* were not present.

2.2 Oxygen Measurements

The water chemistry was consistently recorded by probes in the water column. I used a water meter, YSI 6600 V2 sonde attached with sensors, to measure temperature ($^{\circ}\text{C}$), specific conductivity (mS cm^{-1}), pH, depth (m), and salinity (PSU). The YSI sonde recorded measurements consistently at 15-minute intervals. The YSI 6-series also measured dissolved oxygen (DO, % saturation) at 15-minute intervals. I constructed a stake structure in which I attached the water meter, which I could consistently determine the depth of deployment (~ 0.2 m below water surface, **Figure 8**). I calibrated and deployed the YSI sonde in the ponds at least 1 hour before sampling, in order to mitigate stirring of sediments and particulate matter in the water column. After the completion of every sampling session, I uploaded the recorded data to a computer and checked for battery life. The sensors were regularly inspected, cleaned, and calibrated according to manufacturer specifications. A time series of oxygen concentrations was created to visualize the cyclical nature of oxygen production and consumption in Pond 1.

2.3 Determination of Tidal Flushing

Periods of tidal flushing were indicated by the overtopping of the marsh platform by high tides and the connection to water in the ponds. The frequency of tidal flushing periods was observed via 15-minute tide gauge measurements. The tide gauge station was located at the mouth of the Plum Island sound ($42^{\circ} 42.6\text{N}$, $70^{\circ} 47.3\text{W}$). Measurements recorded by the tide gauge greater than 1.44m NAVD88 (i.e., above the marsh platform) were considered periods of tidal flushing. These periods were confirmed by the measurements from the depth sensor probe on the YSI sonde.

2.4 DIC Measurements

2.4.1 Surface Water

Surface water samples were collected for DIC analysis. A lightweight structure was constructed to be placed on the marsh platform. This would minimize disturbance to vegetation and invertebrate communities during sampling sessions (**Figure 8**). I used a Masterflex E/S portable sampler with $\frac{1}{4}$ inch tubing, making sure the sampling end had a valve and could attach to a 60mL syringe. The intake end of the tube was deployed in close proximity to the YSI probes. I ensured that the tubing was submerged in the pond to keep the temperature of water samples as similar as possible to the temperature of the pond water. I also made sure that tubes did not extend onto the mudflats in order to reduce tubing effects. The number of observations in the two ponds varied due to equipment and temporal limitations. The number of observations of DIC concentrations was relatively fewer than the number of observations of DO concentrations.

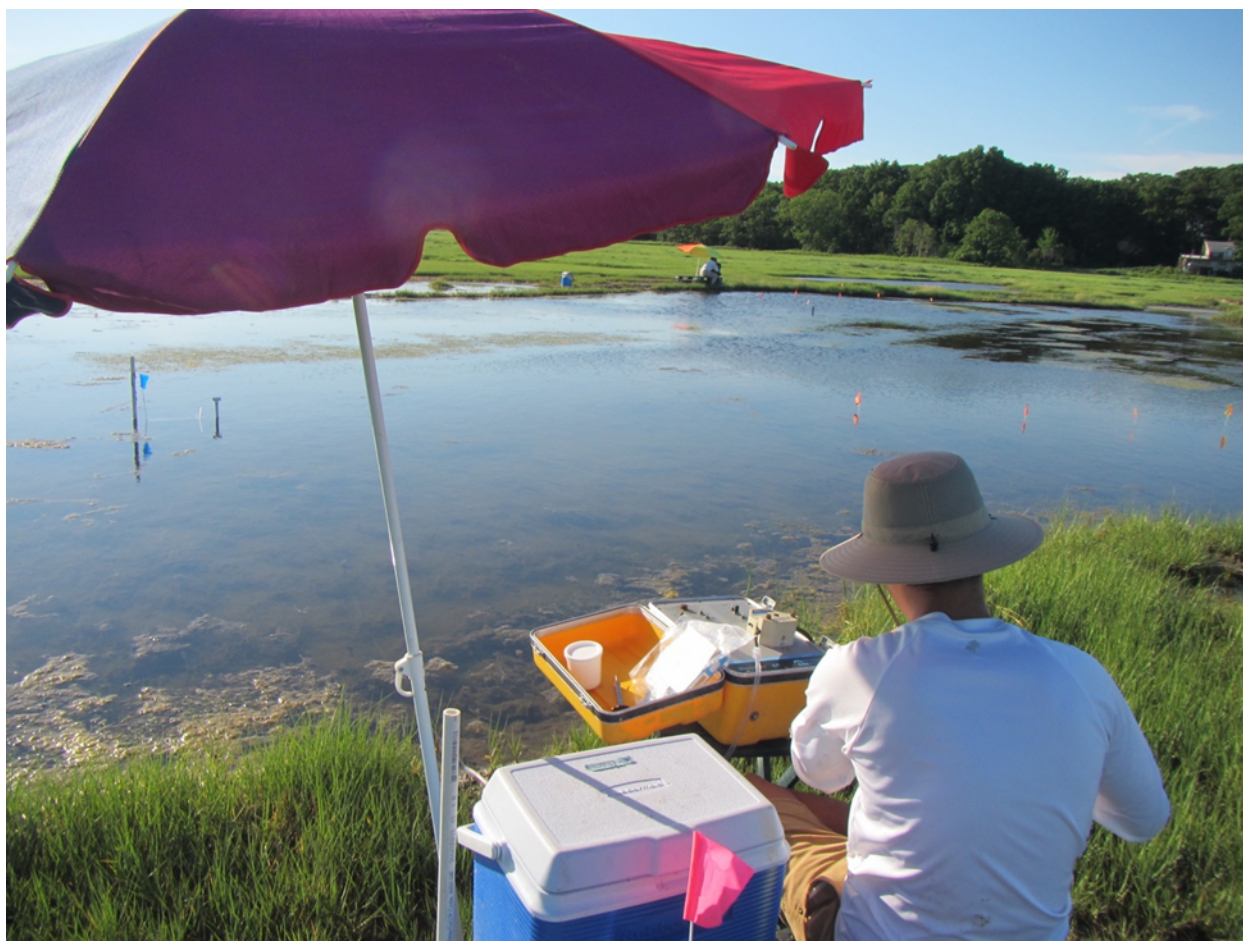


Figure 8. A typical sampling session at Pond 1, taken on July 5, 2017. Portable sampler (yellow) and other equipment are placed on top of a lightweight platform (not pictured). A blue flag (left) indicates position of YSI sonde and sampling intake tube, about 0.22 m below the water surface. Red flags (right) mark locations of transects and porewater sampling. On the other side of the pond, a secondary platform was set up from July 5-6 for a 24-hour sampling session.

2.4.2 Porewater

In addition to collecting surface water samples, I also collected porewater samples during a sampling session on July 5 to July 6, 2017. Porewater samples would also be analyzed for DIC. I intended to see an influx of carbon from the sediments into the pond water. I placed a 1 m² quadrat on the sediment surface about 1 m out from the edge of the pond. I collected four, 5 cm cores from each exterior corner of the quadrat. I combined the materials collected from 2 cores into a single falcon tube immediately after collection and sealed the tube (**Figure 9**). A flag was

placed to indicate the collection location. I continued sampling 1 m away from the flag in a singular direction every 1.5 minutes. Sediment samples were spun in a centrifuge for 5 to 10 minutes, and the separated water was then filtered into an exetainer.

2.4.3 Sediment Cores

I analyzed porewater samples from sediment cores collected by Amanda Spivak's research group from Woods Hole Oceanographic Institute (Spivak et al., 2017). The sediment core was partitioned by layers determined by depth: surface, 0-2 cm, 2-5 cm, 5-8 cm, 8-12 cm, 12-16 cm, 16-20 cm. Porewater was collected from each layer, and I analyzed the DIC concentrations for each layer. Sediment cores for Pond 1 were conducted three times over the study period.



Figure 9. Image of a 5 cm core extracted from each exterior corner of a quadrat. Four cores were combined to a single sampling inside a falcon tube. The tube ran in the centrifuge, and the separated water ran in the DIC analyzer.

2.4.4 Lab Analysis

I analyzed the dissolved inorganic carbon analysis from both surface water samples and pore water samples using the Apollo SciTech Dissolved Inorganic Carbon Analyzer [AS-C3] and controlled via a computer. The analyzer consisted of a LI 7000 solid state infrared CO₂ detector, a mass-flow controller to precisely control carrier gas flow, and a digital pump for transferring small sample volumes.

To analyze the total inorganic carbon in a sample, the machine would add acid, essentially shifting the equilibrium to CO₂. The resulting concentration of partial pressure of CO₂ (pCO₂) was measured and recorded as a representative of DIC. The goal of the measurement is to determine the total amount of inorganic carbon in the sample volume. The sample is acidified to convert the elements to pCO₂. The machine measures the whole emission of pCO₂ from the sample and integrates over the peak to get the total amount. After following the calibration process, samples were analyzed according to manufacturer guidelines: a 1.0 mL of a refrigerated standard was run 3 times, followed by a batch process of each sample, in which 1.0 mL was analyzed 3 times.

The use of the Apollo AS-C3 DIC Analyzer was ideal for utilizing small sample volumes (0.1 to ~1.5 mL). The ability to analyze samples from a small volume assured that there would be results from all time periods regardless of any human or machine error. The AS-C3's built-in infrared CO₂ detector (LI 7000) allowed for an accurate reading after 100% extraction of CO₂ via acidification from the sample within a short period. In the case of error (e.g., incorrect volume of sample, air bubbles in analyzer, fault equipment), some samples were run more than the usual 3 times. An average of each sample's analyzed concentration was taken. The samples,

standards, and other equipment (i.e., syringes, tubing) were kept on ice to ensure consistency during analysis. Porewater samples often had a larger concentration of carbon, and thus a smaller injection volume was used (< 0.8 mL, depending on depth of collection). There were instances in which the Apollo Analyzer malfunctioned because of high particulate matter in pore water sample vials, and some samples could be analyzed less than 3 times.

2.5 Metabolic Rates

2.5.1 Net Ecosystem Production, Respiration, and Gross Primary Production

I used a whole system approach to determine metabolic rates, because the concentration change of oxygen ($\Delta O_2 / \Delta t$) or DIC ($\Delta DIC / \Delta t$) in the pond surface water reflects processes occurring in the sediment and in the water column (**Figure 10, 11**). In addition, pond-atmosphere exchange has to be considered.

$$\frac{\Delta O_2}{\Delta t} = NEP + Flux_{atm}$$

$$\frac{\Delta DIC}{\Delta t} = NEP + Flux_{atm}$$

$$NEP = R - GPP$$

where GPP, NEP, and R are in $\text{mmol m}^{-2} \text{h}^{-1}$. NEP is the amalgam of the rates of respiration (R) and production (GPP). Essentially, the analyzed concentrations of DIC from surface water samples encompass not only the component from the water column, but also the flux component from the sediment. The measured DIC does not however take into account fluxes between the pond surface and the atmosphere. The rate of NEP can be understood as the sum of the change in DIC and the atmospheric flux of DIC.

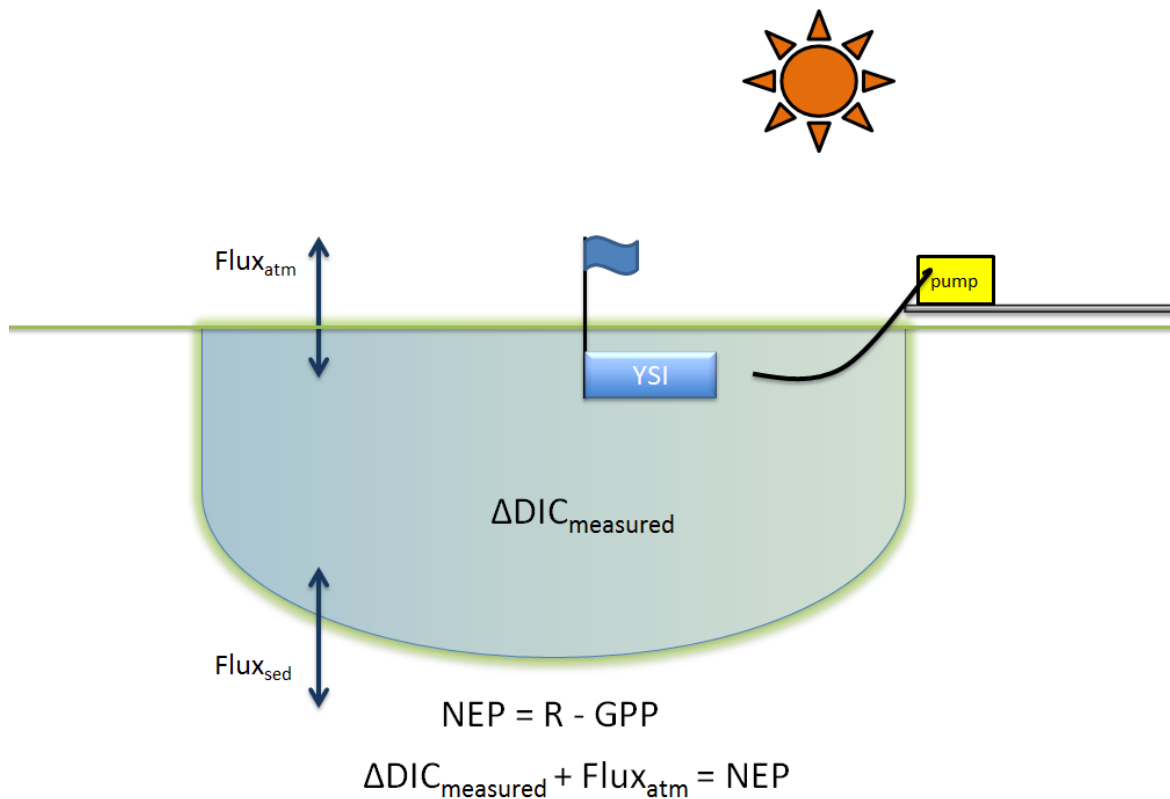


Figure 10. Diagram explaining the components of DIC in pond water during daytime measurements. Fluxes from the sediment and atmosphere are labeled, as well as equations that explain calculation of gross primary production (GPP), net ecosystem production (NEP), and respiration (R).

To partition net ecosystem production in the two component fluxes respiration and gross primary production, I assume that NEP at night equals respiration.

2.5.2 Differences in Day and Night

In the absence of sunlight during nighttime, I assumed no photosynthetic activity would occur in the pond (**Figure 11**). Without the component of GPP, I could simplify the equation of NEP to equal R. Thus, I estimated for respiration occurring at night (R_{night}) as a sum of the

measured DIC or oxygen concentration change and the atmospheric flux. The nighttime period was defined as PAR (photosynthetically active radiation) $< 10 \mu\text{mol m}^{-2} \text{s}^{-1}$ and further constrained to 20:15 to 3:15 local time. The rate of respiration was assumed to stay constant throughout the day.

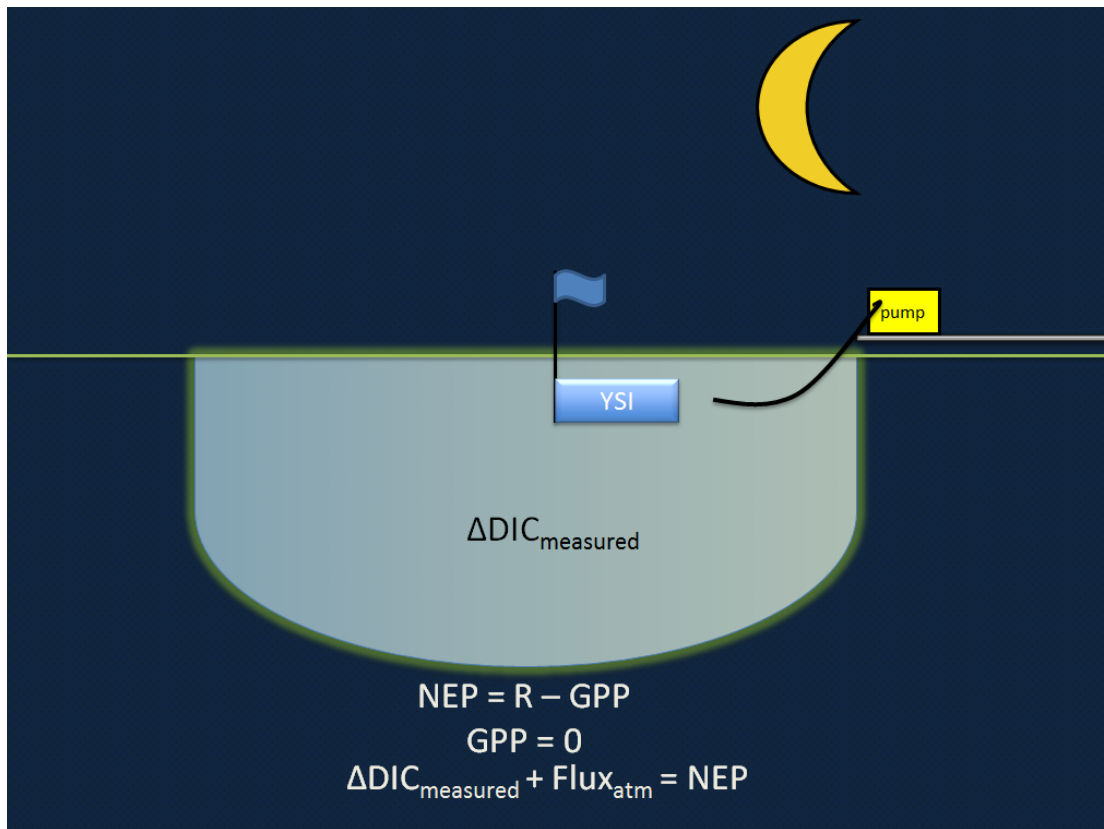


Figure 11. Diagram explaining the components of DIC in pond water during daytime measurements. Equations that explain calculation of gross primary production (GPP), net ecosystem production (NEP), and respiration (R) are labeled.

2.5.3 Atmospheric Flux

The general equation describing the flux between an aquatic system and the atmosphere is given by:

$$\text{Atmospheric Flux} = k * (c_w - \alpha * c_a)$$

where k is the gas transfer velocity, c_w the concentration in water, c_a the concentration in air, and α is a solubility coefficient.

I estimated k using the parameterization by Vachon and Prairie (2013), which as been shown to work best in these pond systems (Howard, 2017):

$$k = 2.51 + 1.48 \times U10 + 0.39 \times U10 \times \log_{10} LA$$

where LA is lake area (or pond area in this case) in km^2 , and $U10$ is wind speeds at 10 meters.

Wind speeds (U) measured at 14 m from eddy covariance towers were scaled to 10 m height above the water surface (Winslow, 2006).

To estimate the concentration gradient of CO_2 , I calculated pCO_2 concentration using the DIC concentrations and pH, and used the atmospheric measurements of CO_2 . To estimate the concentration gradient of oxygen, I calculated the saturation concentration of oxygen in the water using sonde data and assumed that the atmosphere was saturated in oxygen (100%).

$$\text{gas flux}_{DO} = \left[DO - \left(\frac{DO}{DO\%} * 100 \right) \right] * k$$

where DO concentrations is in mg L^{-1} , depth in m, gas flux in $\text{g m}^{-2} \text{min}^{-1}$, and k in m min^{-1} .

Gas transfer velocities (k ; m d^{-1}) were adjusted using a Schmidt number of 600 (Wanninkhof, 2014). The Weiss solubility constant for CO_2 in seawater (k_0 , $\text{moles L}^{-1} \text{atm}^{-1}$) was calculated and corrected for salinity and temperature.

2.5.4 Oxygen-based Calculations

Dissolved oxygen saturation concentration was calculated. Gas flux of oxygen in $\text{g m}^{-2} \text{min}^{-1}$ was found using k and the difference between saturation concentration and measured concentration, and the gas flux was corrected for the depth of the YSI sonde (0.22 m). The exchange of oxygen was calculated as a function of concentration and sonde depth

$$R_{DO} = \frac{\Delta DO}{depth * 15} - gas\ flux_{DO}$$

$$gas\ flux_{DO} = \left[DO - \left(\frac{DO}{DO\%} * 100 \right) \right] * k$$

where DO concentrations is in mg L^{-1} , depth in m, gas flux in $\text{g m}^{-2} \text{min}^{-1}$, and k in m min^{-1} .

Two different rates of pond metabolism were calculated: one for days with conditions of tidal isolation and one for days with conditions of tidal flushing.

The rates of metabolism for daily averages were calculated.

2.5.5 DIC-based Calculations

An average rate of R was calculated from R_{night} values of each sampling session. During daytime periods, GPP was calculated as the difference of NEP and R . Estimates of GPP, NEP, and R were corrected for pond surface area. The rates of metabolism for daily averages were calculated.

3. Results

3.1 Pond 1

3.1.1 Environmental Conditions

The study area encompassed the pond and surrounding marshland. The pond had a surface area of 931m² and an estimated volume of 307.23 m³ (**Figure 4**). The main primary producers in the pond were surface water and sediment microalgae, submerged grass *R. maritima*, and the macroalgae *Ulva* (**Figure 6**).

Weather conditions during the study months of June to August, precipitation was 0.23 cm. Water temperatures ranged from 16.8°C to 32.57°C but were warmer during isolated tidal periods. Temperature and salinity differences between tide stages were stronger in the summer (Spivak et al., 2017).

Temperature measurements in Pond 1 ranged from 16.8°C to 32.57°C, with an average of 24.48°C (**Figure 13**). Salinity ranged from 12.12 ppt to 29.54 ppt. Specific conductivity measurements ranged from 20.23 mS/cm to 45.67 mS/cm. During the first deployment of the sonde (June 14-20), pH measurements ranged from 8.28 to 9.30 (**Figure 12**). After the spring tide period (June 30-July 5), pH ranged from 8.15 to 9.43. During the spring tide period (June 20-29), pH ranged from 7.06 to 9.10.

3.1.2 Periods of Tidal Flushing

Periods of tidal flushing that were initially indicated with measurements of the tide gauge measurements were confirmed with the depth measurements of the water meter (**Figures 12, 13**). A delay of about 75 minutes between the indications of the tide gauge and the indications of the water meter occurs. The constant offset represents the amount of time passed for seawater to traverse through creeks and eventually overtop the marsh landscape. There were in total 21 days of tidal inundation observed during the study period. The first indication of tidal inundation was observed to be on June 20 at 20:30 to 21:45. There were 10 days with only nighttime inundation.

There was 1 day with only daytime inundation. There were 5 days with both daytime and nighttime inundation, from June 23 to June 28. Days with both daytime and nighttime inundation occurred consecutively. There appeared to be a period of time from June 20 to June 29, where there were concentrated instances of tidal inundation. There were 15 of the 21 instances of tidal inundation in just these 10 days. This period of concentrated tidal flushing matches characteristics of spring tide conditions.

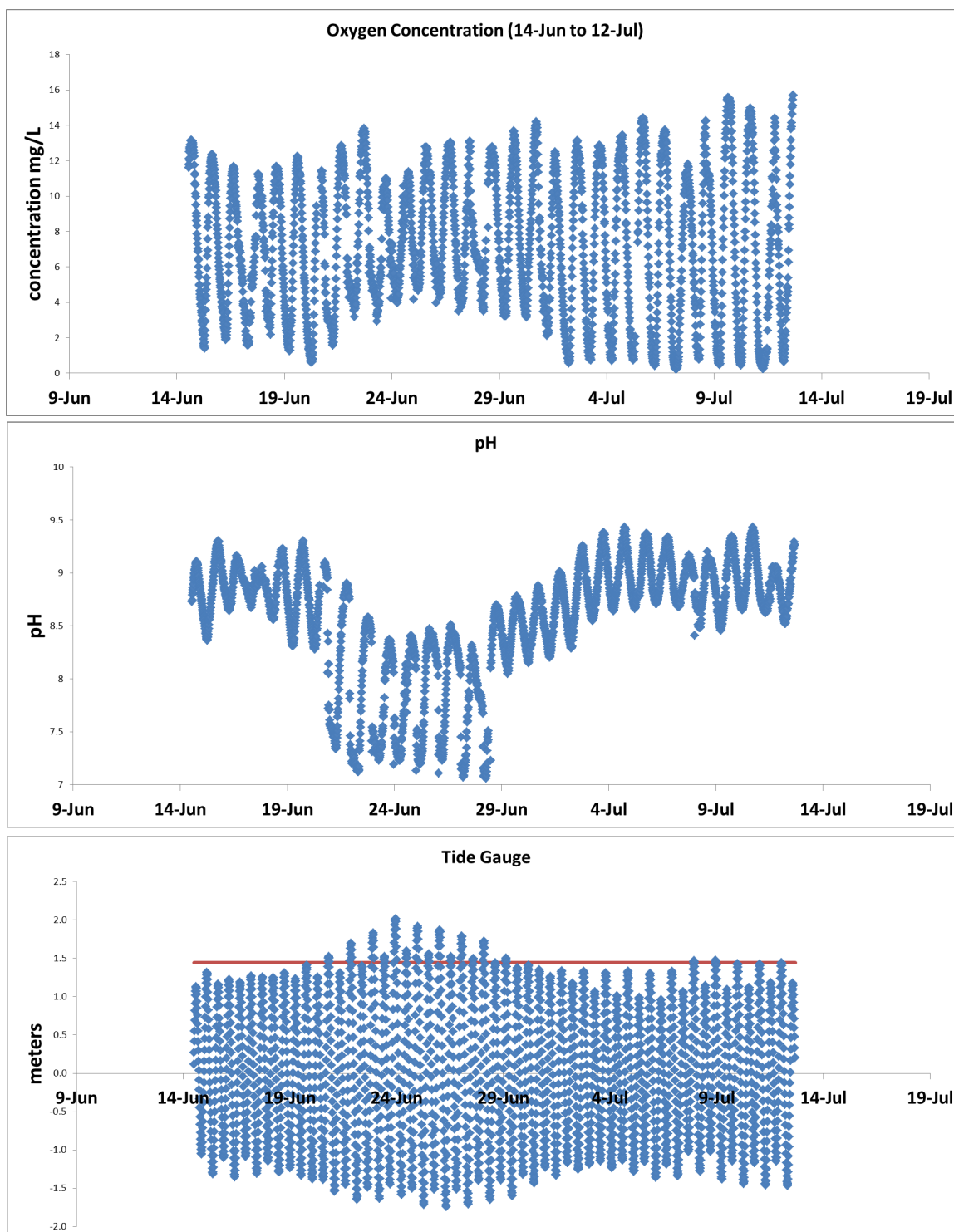


Figure 12. Observations of oxygen and pH collected by the YSI sonde, as well as tide gauge measurements are displayed from mid-June to mid-July, 2017. These categories were continually recorded in 15-minute intervals. Fluctuations of each measurement throughout a diurnal cycle can be shown. A period of concentrated tidal flushing (i.e., spring tide conditions) is defined to be from June 20 to June 30. It is indicated by a decrease in fluctuations of oxygen concentrations, an overall decrease in pH, and increase in fluctuations in tide gauge measurements. Tide gauge data points above the 1.44 m NADV88 (red line) indicate flooding at the mouth of Plum Island Estuary.

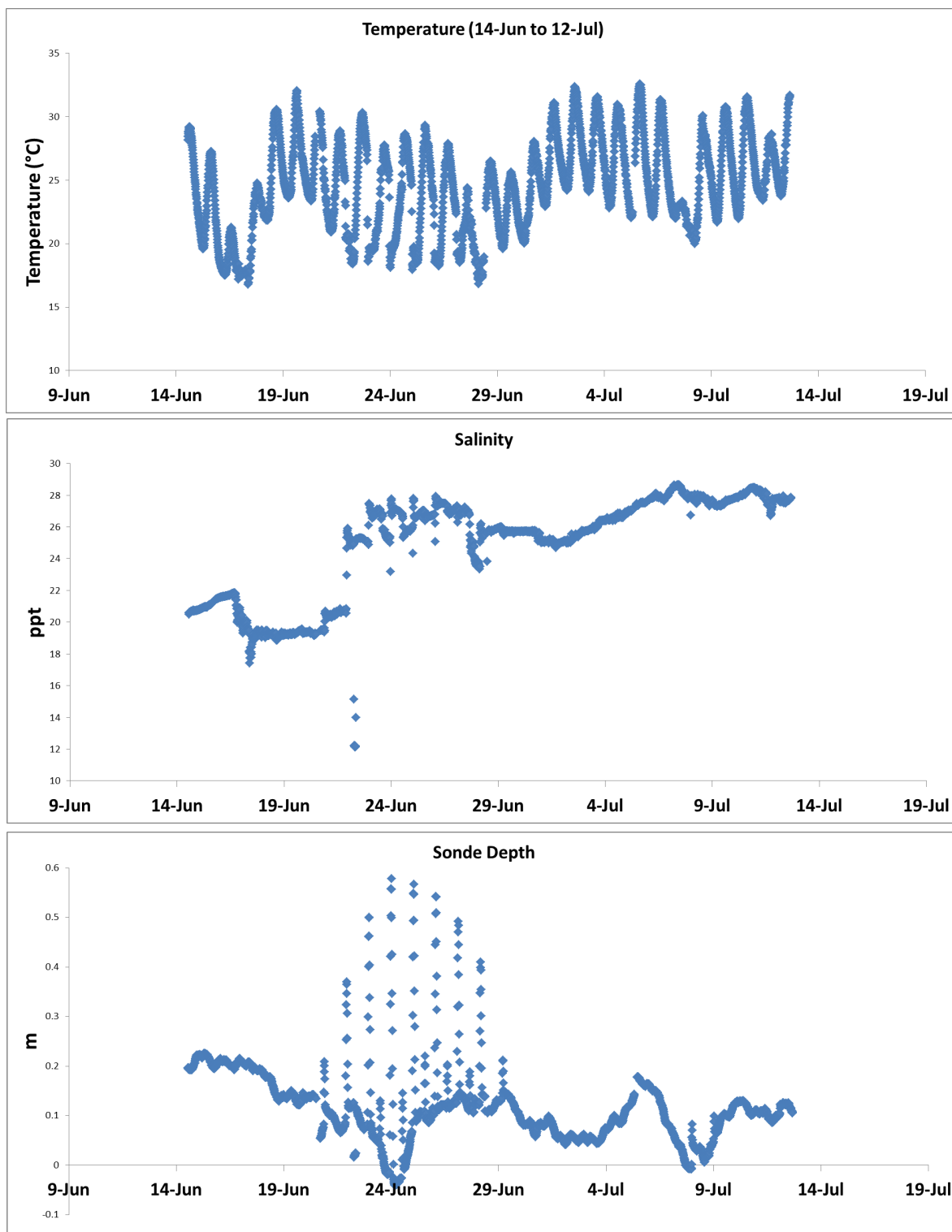


Figure 13. Observations of temperature, salinity, and depth collected by the YSI sonde from mid-June to mid-July, 2017. These categories were continually recorded in 15-minute intervals. Fluctuations of each measurement throughout a diurnal cycle can be shown. A period of concentrated tidal flushing (i.e., spring tide conditions) is defined to be from June 20 to June 30. It is indicated by an increase in overall salinity and an increase in fluctuations of depth measurements.

3.1.3 Oxygen Concentrations

Oxygen concentrations were measured for 37 days in Pond 1. The number of observations in the two ponds varied due to equipment and temporal limitations. Throughout the summer, dissolved oxygen concentrations in Pond 1 ranged from 0.23 mg L^{-1} to 19.52 mg L^{-1} (**Figure 12**). In the study, hypoxic conditions were defined when most oxygen is consumed at salinities between 35 and 20 ppt (i.e., $\text{DO} < \sim 2.0 \text{ mg L}^{-1}$) [Melzner et al., 2012, Timmerman and Chapman, 2004].

During the entirety of the study, hypoxic conditions occurred on 23 (59%) nights in the pond. Occurrences of hypoxic conditions varied with tide stage; the occurrence of hypoxia in Pond 1 was 4.44 times greater during periods of tidal isolation (21 out of 26 nights) than inundation (2 out of 11 nights). The pond frequently reached hypoxic conditions during periods of tidal isolation from July to August relative to periods of tidal inundation. Dissolved oxygen concentrations ranged from 0.62 to 13.15 mg L^{-1} with an average of 6.81 mg L^{-1} in first deployment of the YSI sonde, which happened to also be before the period of concentrated tidal inundation (June 14-20, **Figure 14**). DO concentrations ranged from 0.43 mg L^{-1} to 14.41 mg L^{-1} during the several days after the period of concentrated tidal inundation (June 30-July 5). During the period of concentrated tidal inundation (June 20-29, **Figure 15**), concentrations ranged from 1.58 mg L^{-1} to 13.82 mg L^{-1} . During spring tide conditions, the daily peaks in oxygen were usually lower compared to peaks during tidal isolation. However, during spring tide conditions, oxygen dipped to a lesser extent compared to dips during tidal isolation. There are some data points in which DO concentrations were affected by weather conditions (i.e., clouds, rain) as seen in days like June 17th.

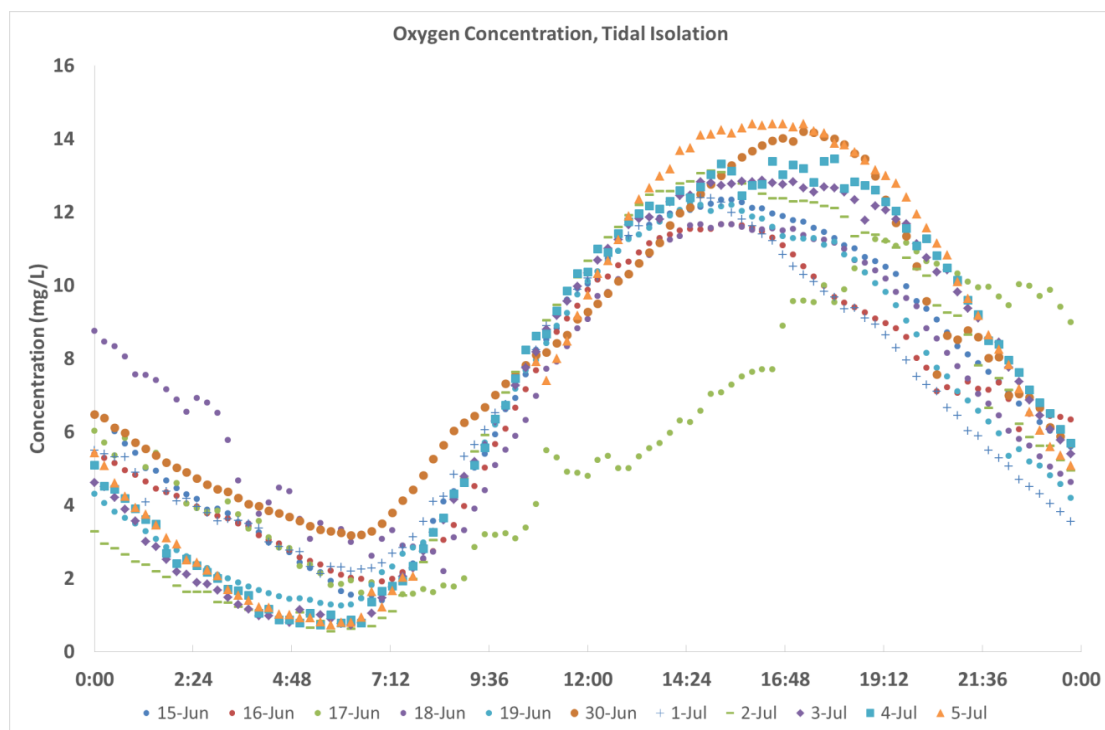


Figure 14. Time series of dissolved oxygen concentrations during days of tidal isolation (i.e., no flooding) in Pond 1.

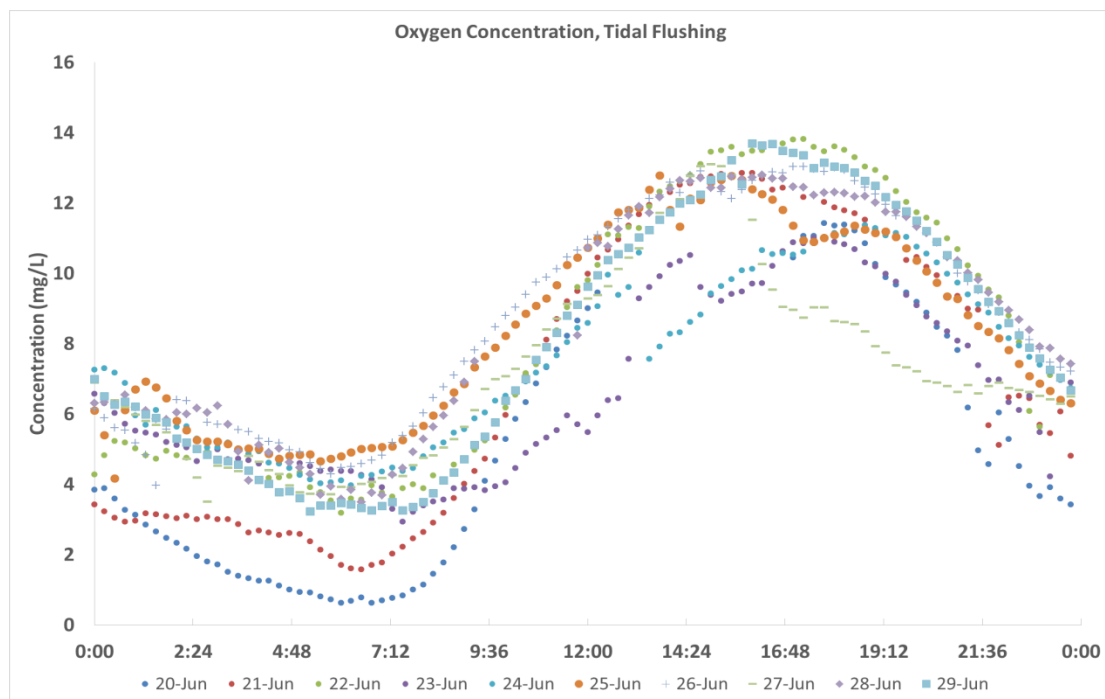


Figure 15. Time series of dissolved oxygen concentrations during days of tidal flushing in Pond 1. Note that with the exception of June 20 and 21, the pond's oxygen concentrations rarely dip below 4 mg L^{-1} .

3.1.4 DIC Concentrations

3.1.4.1 Surface Water Samples

Concentrations of dissolved inorganic carbon (DIC) were calculated for 5 sampling sessions. During Session 1, DIC concentrations ranged from 1065.06 $\mu\text{mol L}^{-1}$ to 2039.28 $\mu\text{mol L}^{-1}$. During Session 2, concentrations ranged from 1390.63 $\mu\text{mol L}^{-1}$ to 1833.66 $\mu\text{mol L}^{-1}$. During Session 3, concentrations ranged from 974.39 $\mu\text{mol L}^{-1}$ to 1731.74 $\mu\text{mol L}^{-1}$. During Session 4, concentrations ranged from 1190.57 $\mu\text{mol L}^{-1}$ to 2161.97 $\mu\text{mol L}^{-1}$. Overall, DIC concentrations in Pond 1 ranged from 974.39 $\mu\text{mol L}^{-1}$ to 2161.94 $\mu\text{mol L}^{-1}$ (**Figure 16**). The period of spring tide conditions occurred between Session 1 and Session 2. DIC concentrations followed a general diurnal pattern: concentrations decreased during photosynthesis occurring during the day, and concentrations increased during the absence of photosynthesis and the overtaking of respiration at night.

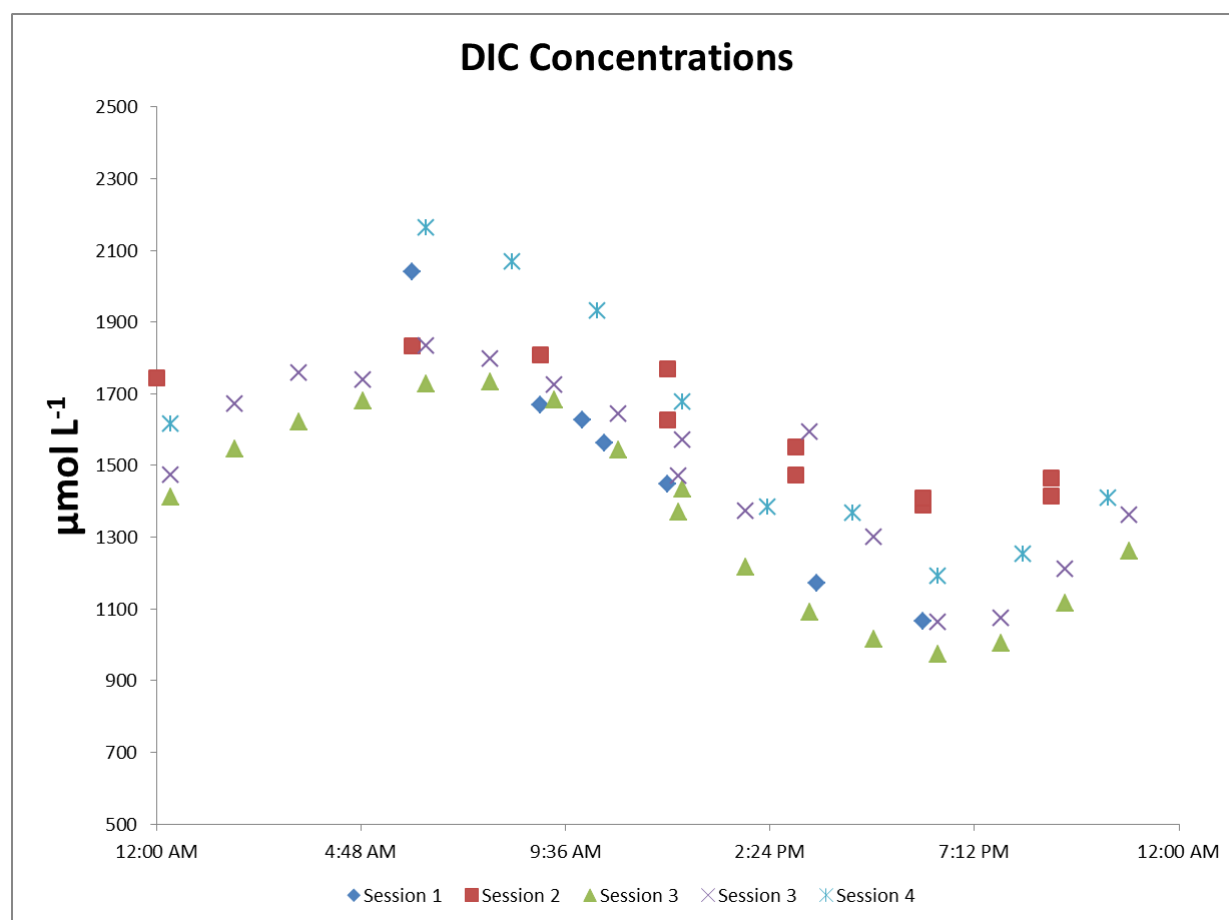


Figure 16. Time series of dissolved inorganic carbon (DIC) concentrations analyzed from four sampling sessions in Pond 1. There were two sets of samples collected during Session 3 (July 5-6) as part of a joint session with members from WHOI.

3.1.4.2 Overnight Porewater Samples

Concentrations of DIC from July 5 to July 6 were measured in two locations in Pond 1. The concentrations of DIC in the first site ranged from 5791.59 $\mu\text{mol L}^{-1}$ to 15203.94 $\mu\text{mol L}^{-1}$, with an average of 9556.6 $\mu\text{mol L}^{-1}$ for the session. The concentrations of DIC in the second site ranged from 4581.88 $\mu\text{mol L}^{-1}$ to 14645.96 $\mu\text{mol L}^{-1}$, with an average of 8029.6 for the session.

3.1.4.3 Sediment Cores

Throughout the three time points in which collection of sediment cores were conducted, the concentration of DIC ranged from 993.57 $\mu\text{mol L}^{-1}$ (on the surface) to 21219.40 $\mu\text{mol L}^{-1}$ (16-20 cm below surface) [Table 1]. An average concentration value was calculated for each depth layer (Figure 17). On the surface level, the average concentration of DIC was 1407.37 $\mu\text{mol L}^{-1}$ and in Layer 6, the average concentration was 17440.15 $\mu\text{mol L}^{-1}$. Thus we see an increase in concentration with depth.

Table 1. Results from porewater analysis. Sediment cores collected by members of WHOI. Concentrations of DIC from sediment cores were analyzed for each time point. An average concentration for each sediment depth layer is displayed on the right.

Name	Depth	Time Point 1	Time Point 2	Time Point 3	Avg Concentration
	cm	$\mu\text{mol L}^{-1}$	$\mu\text{mol L}^{-1}$	$\mu\text{mol L}^{-1}$	$\mu\text{mol L}^{-1}$
Surface	0	993.57	1649.08	1579.45	1407.37
Layer 1	0-2	6470.55	5121.14	5138.44	5576.71
Layer 2	2-5	9750.57	8056.92	6330.28	8045.92
Layer 3	5-8	9941.89	11424.74	10742.38	10703.00
Layer 4	8-12	12626.05	12407.45	18516.32	14516.61
Layer 5	12-16	13993.34	13790.66	20479.55	16087.85
Layer 6	16-20	15079.64	16021.42	21219.40	17440.15

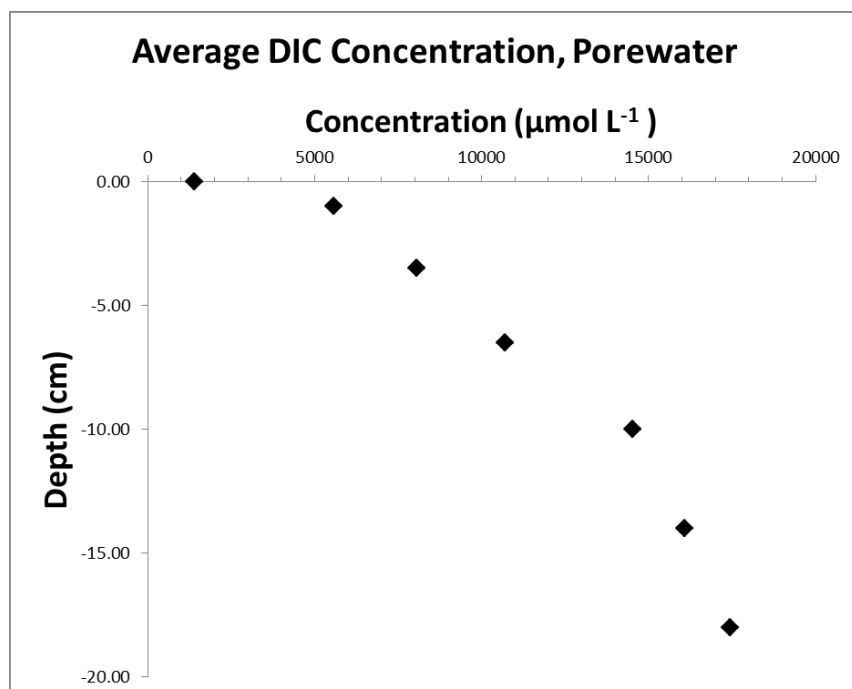


Figure 17. Results from DIC analyses of sediment cores provided by A. Spivak of WHOI. An average of three time points was displayed for each depth layer.

3.1.5 Metabolism – Oxygen

The average rate of respiration based on DO concentrations was estimated at $16.98 \text{ mmol m}^{-2} \text{ hr}^{-1}$. The average rate of respiration during periods of tidal isolation (i.e., June 15-19, July 4-12) was estimated at $7.15 \text{ mmol m}^{-2} \text{ hr}^{-1}$. The average rate of respiration during periods of tidal flushing (i.e., June 20-29) was estimated at $4.70 \text{ mmol m}^{-2} \text{ hr}^{-1}$. There was particular focus of respiration rates during nights of June 23, 34, and 25. Due to tidal flushing during the nighttime, oxygen concentrations increased. This resulted in a nighttime peak in the concentrations of oxygen (**Figure 18**). R_{night} was estimated to be $2.70 \text{ mmol m}^{-2} \text{ h}^{-1}$, $3.08 \text{ mmol m}^{-2} \text{ h}^{-1}$, and $4.01 \text{ mmol m}^{-2} \text{ h}^{-1}$ for the remainder of the nighttime following the second peak of oxygen concentrations on June 23, June 24, and June 25, respectively (i.e., respiration rates calculated

after 1:15 EST). The average rate of R_{night} for these three dates was $3.27 \text{ mmol m}^{-2} \text{ h}^{-1}$. In comparison, the average rate of R_{night} during the same timeframe for dates without tidal flushing (i.e., respiration rates calculated after 1:15 EST for June 16-20) was $1.27 \text{ mmol m}^{-2} \text{ h}^{-1}$.

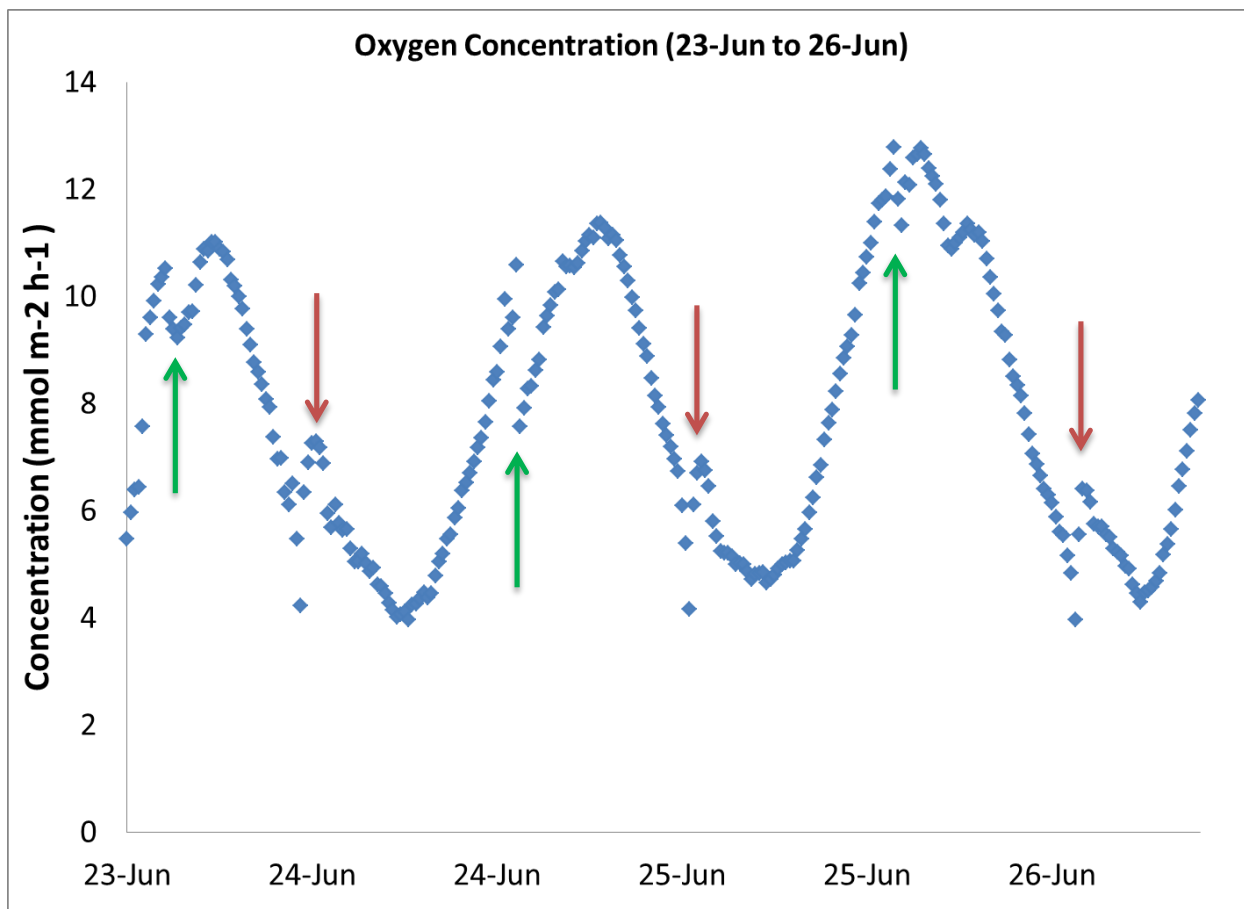


Figure 18. Time series of dissolved oxygen concentration from June 23 to 26. Red arrows indicate a second peak of oxygen concentrations due to an influx of oxygen from surrounding creeks during periods of nighttime tidal flushing. Green arrows indicate a dip in oxygen concentrations due to dilution effects from incoming water from surrounding creeks during periods of daytime tidal flushing.

3.1.6 Metabolism – DIC

The average rate of respiration based on DIC concentrations was estimated to be 27.29 $\text{mmol m}^{-2} \text{hr}^{-1}$. Again, the rate of respiration was assumed to stay constant throughout the diurnal cycle.

During Session 1, the average rate of GPP was estimated at 8.64 $\text{mmol m}^{-2} \text{hr}^{-1}$. The corresponding average rate of NEP was estimated at 39.58 $\text{mmol m}^{-2} \text{hr}^{-1}$. During Session 2, the average rate of GPP was estimated at 29.79 $\text{mmol m}^{-2} \text{hr}^{-1}$. The corresponding average rate of NEP was estimated at 2.50 $\text{mmol m}^{-2} \text{hr}^{-1}$. During Session 3, the average rate of GPP was estimated at 37.83 $\text{mmol m}^{-2} \text{hr}^{-1}$. The corresponding average rate of NEP was estimated at -3.11 $\text{mmol m}^{-2} \text{hr}^{-1}$. During Session 4, the average rate of GPP was estimated at 120.31 $\text{mmol m}^{-2} \text{hr}^{-1}$. The corresponding average rate of NEP was estimated at 93.01 $\text{mmol m}^{-2} \text{hr}^{-1}$. During Session 5 (Pond 2), the average rate of GPP was estimated at -25.20 $\text{mmol m}^{-2} \text{hr}^{-1}$. The corresponding average rate of NEP was estimated at -25.54 $\text{mmol m}^{-2} \text{hr}^{-1}$.

3.1.7 Comparison of Rates – Oxygen and DIC

The changes in concentrations of DIC seem to mirror the changes in concentrations of oxygen, but they show a similar temporal dynamic than oxygen (**Figure 19**). During the daytime, concentrations of oxygen are observed to increase and concentrations of DIC are observed to decrease simultaneously. During the nighttime, oxygen decreases while DIC increases.

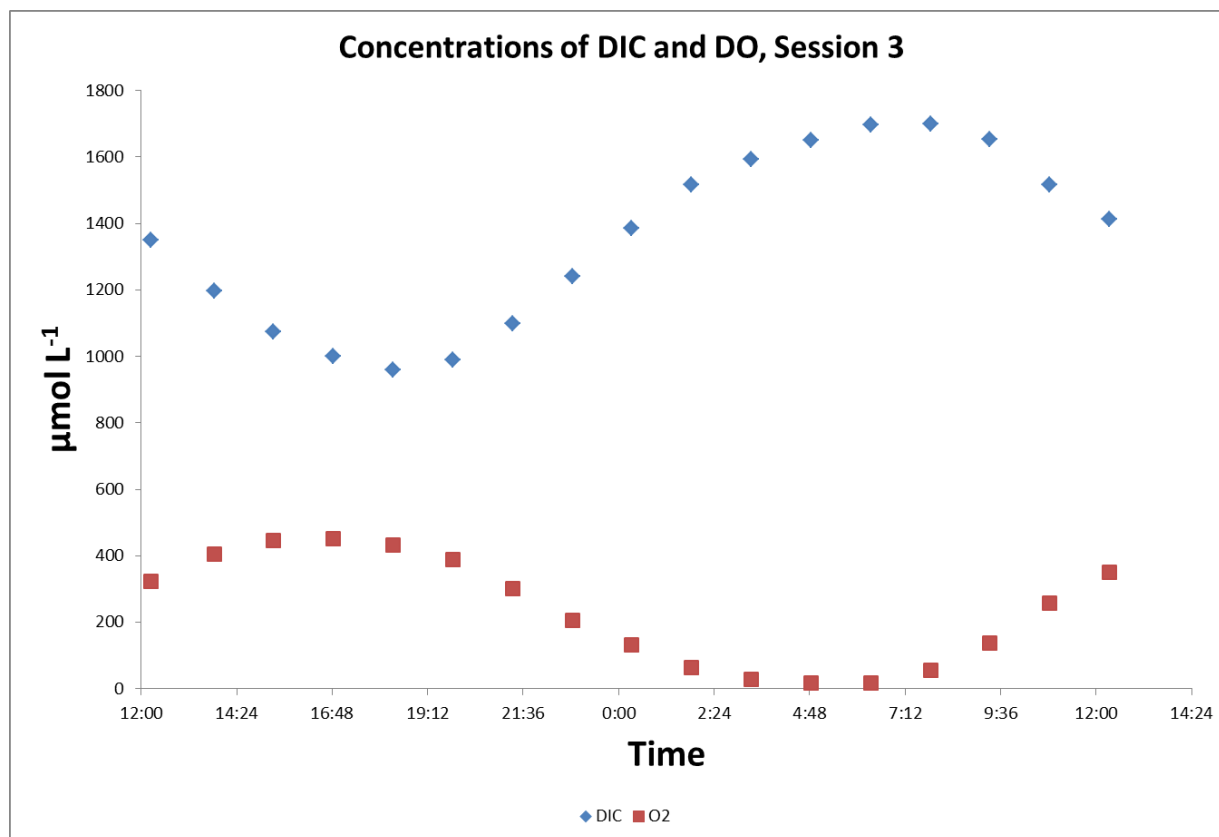


Figure 19. Time series displaying concentrations of oxygen and DIC during Session 3 (July 5-6). This graph shows the dynamics of inorganic carbon and oxygen concentrations without effects of tidal flushing (i.e., nighttime influx, daytime dilution). During the day, oxygen increases and DIC decreases (due to photosynthesis). During the night, oxygen decreases and DIC increases (due to rates of respiration > rates of photosynthesis).

Comparisons of changes in DO concentrations and DIC concentrations (**Figure 20**) display the relationship between the two metrics following a 1:1 correspondence, with exceptions on the left and right. The extreme values, in which the changes in DIC concentrations correspond to disproportionate changes in DO concentrations, are denoted as periods of high productivity (negative X-values) and periods of hypoxia or anoxia (positive X-values). It is during these periods that our oxygen-based estimated rates of metabolism underestimate the true rates of metabolism.

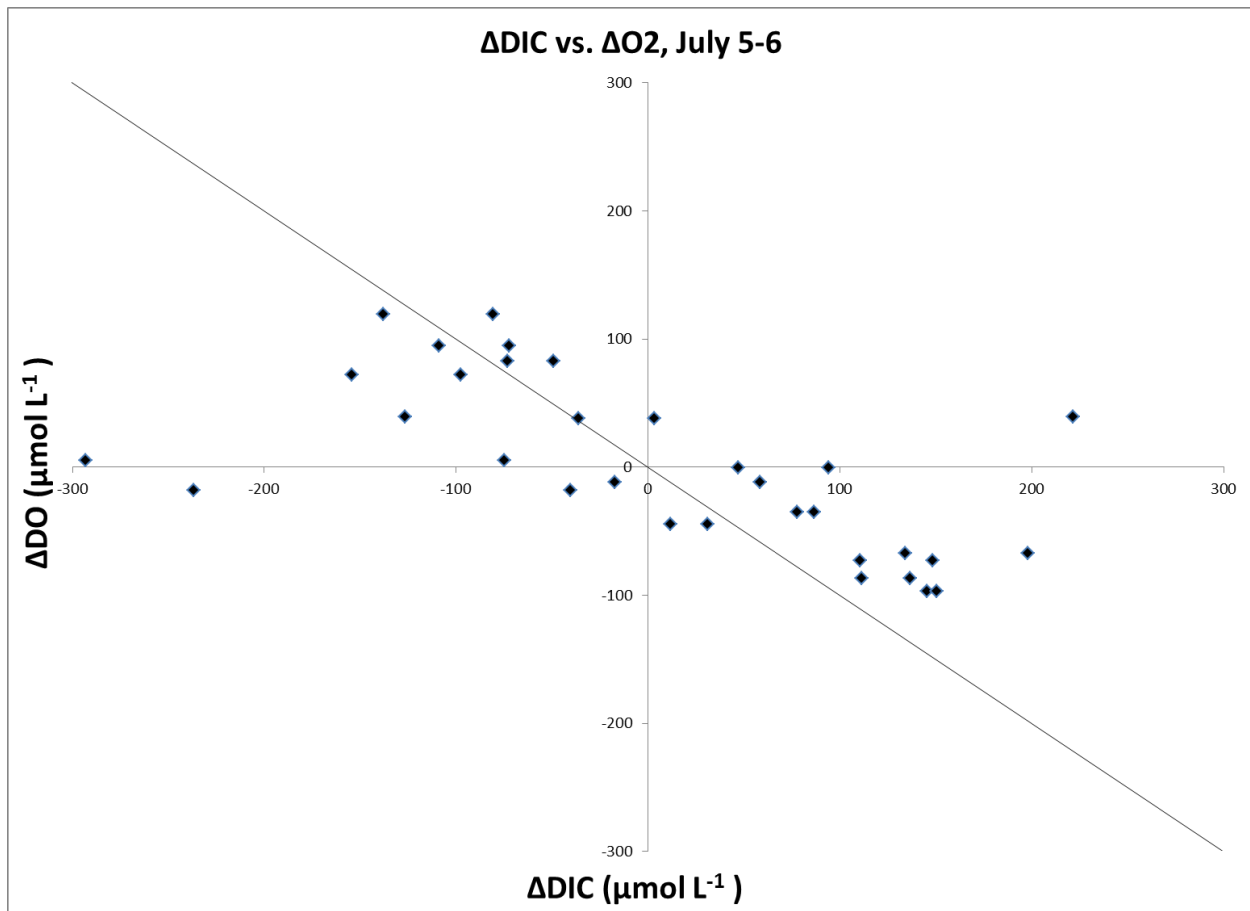


Figure 20. A plot displaying change in concentrations of DIC versus change in concentrations oxygen. Concentrations displayed are from Pond 1, July 5-6. Note that most of the data points follow a 1:1 correspondence, with exceptions in times of high productivity and times of hypoxic conditions in the pond.

Daily averages of GPP, NEP, and R of Pond 1 were calculated for both measurements of dissolved oxygen and dissolved inorganic oxygen (**Figure 21**), and I observed that there were differences in magnitude. The daily average rates of GPP, NEP, and R based on DO were $22.45 \text{ mmol m}^{-2} \text{ hr}^{-1}$, $5.48 \text{ mmol m}^{-2} \text{ hr}^{-1}$, $-16.98 \text{ mmol m}^{-2} \text{ hr}^{-1}$. The daily average rates of GPP, NEP, and R based on DIC were $58.44 \text{ mmol m}^{-2} \text{ hr}^{-1}$, $31.15 \text{ mmol m}^{-2} \text{ hr}^{-1}$, and $-27.29 \text{ mmol m}^{-2} \text{ hr}^{-1}$.

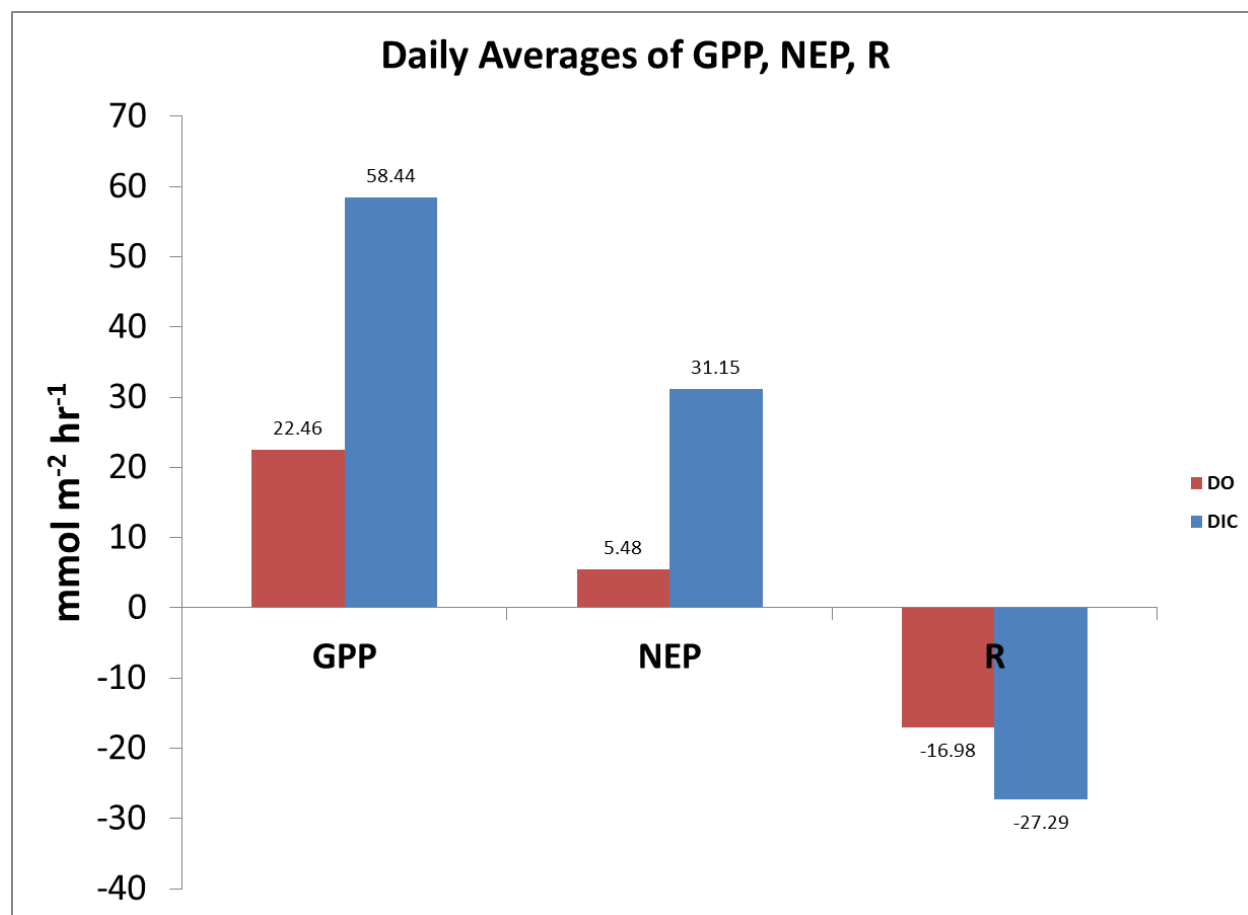


Figure 21. The estimated daily average rates of gross primary production (GPP), net ecosystem production (NEP), and respiration (R). Oxygen-based rates are displayed in red, and DIC-based rates are displayed in blue. Oxygen-based rates are lower than DIC-based rates.

3.2 Pond 2

The pond had a surface area of 26.34 m² and an estimated volume of 8.69 m³. The main primary producers in the pond were surface water and sediment microalgae. The pond did not contain any *R. maritima* or *Ulva* communities.

Weather conditions during the study period of Pond 2 was cloudy, with a temperature range of 17.78 °C to 28.89 °C. Water temperatures ranged from 23.61 °C to 29.94 °C, with an

average of 26.29 °C. Salinity ranged from 28.87 ppt to 29.04 ppt. Specific conductivity ranged from 23.61 mS cm⁻¹ to 29.94 mS cm⁻¹. pH ranged from 7.26 to 8.42.

During Session 5 (August 2 to 3), the only sampling session in Pond 2, concentrations ranged from 2137.23 μmol L⁻¹ to 2676.91 μmol L⁻¹.

Daily averages of GPP, NEP, and R were calculated for Ponds 1 and 2 (**Figure 22**). The daily average rates of GPP, NEP, and R for Pond 1 were 58.44 mmol m⁻² hr⁻¹, 31.15 mmol m⁻² hr⁻¹, and -27.29 mmol m⁻² hr⁻¹, respectively. The daily average rates of GPP, NEP, and R for Pond 2 were 8.40 mmol m⁻² hr⁻¹, -8.51 mmol m⁻² hr⁻¹, and -16.91 mmol m⁻² hr⁻¹, respectively. It is important to note that there are only two days of measurements in Pond 2 and 27 days in Pond 1. It is also important to note that the measurements taken at Pond 1 and Pond 2 are not simultaneous measurements at both sites. There is a difference of 6 days between the last measurements of Pond 1 and the measurements at Pond 2.

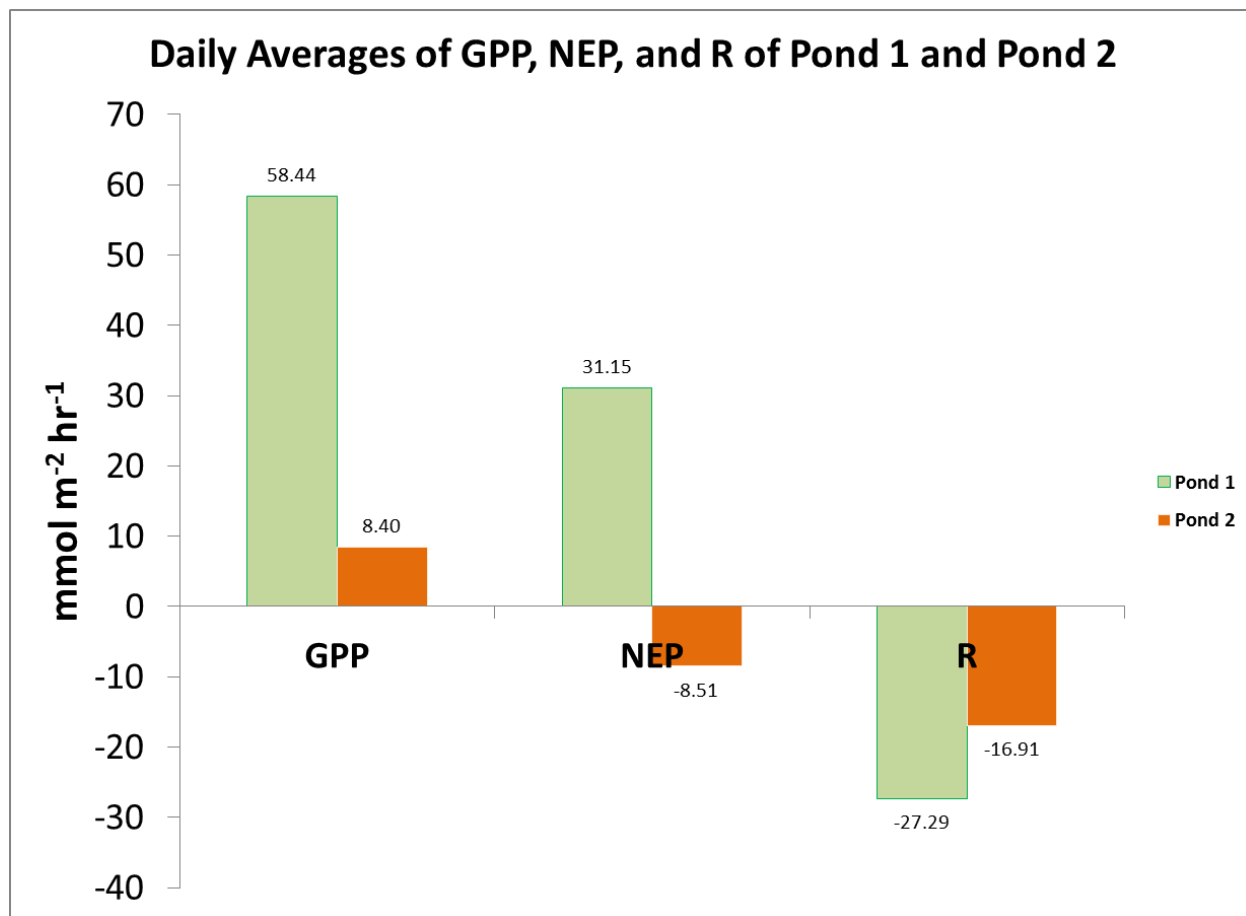


Figure 22. The estimated daily average rates of gross primary production (GPP), net ecosystem production (NEP), and respiration (R). Estimated rates of metabolism are based on DIC concentrations. Rates of metabolism for Pond 1 are displayed in green, and rates of metabolism for Pond 2 are displayed in orange.

4. Discussion

4.1 Estimation of Respiration in Salt Marsh Ponds

Similar to Spivak et al. (2017), I found that changes in oxygen concentrations vary largely between day and night. Nighttime hypoxia was frequently observed. Under the period of tidal flushing, the two metrics – oxygen and DIC – show a reasonable agreement for metabolic rates, except for periods of very low oxygen concentrations at night. This confirms my

assumptions stated earlier and shows that oxygen-based rates of GPP, NEP, and R result in an underestimation of the true rates of respiration.

The determination of periods of tidal flushing and the estimates of metabolic rates presented here represent an attempt to characterize the roles of ponds in salt marshes. During the duration of the study, tidal flushing occurred most frequently in late-June (June 20-29). This is because a perigean spring tide was occurring at this time (NOAA, 2017), when the moon is either near or full and closest to earth. During this time, higher than normal high tides and lower than normal low tides occurred. The tides would have increased near the June 21 summer solstice, due to the position of the sun relative to the earth's equator. Mean sea level was also typically higher due to changing weather patterns and increasing water temperatures.

The selection of Pond 1 and Pond 2 as my study sites was contingent on several factors. Pond 1 and Pond 2 were located on the high marsh, where the marsh platform does not flood daily, but rather during periods of intense fluctuations in tides. Pond 1 and other nearby ponds within the high marsh have also been previously studied by contributors and scientists of the PIE-LTER project (Spivak et al., 2017; Kearns et al., 2017; Johnston et al., 2003). Pond 1 and Pond 2 were also chosen due to limitations in accessibility. The ponds were in close proximity to one another and at similar elevations in the high marsh. They varied in surface area, but also had different plant and algal communities. The ponds that I could study had to be accessible by vehicle and foot, especially when carrying sampling equipment and platforms.

My measurements during sampling Session 3 show that oxygen-based respiration indeed underestimates true rates of respiration when compared to the DIC-based estimates. This occurs primarily during hypoxic conditions [**Figure 20**]. During the study period, it seems that tidal

isolation would create conditions that would stimulate higher rates of respiration (e.g., warmer temperatures, higher daytime concentrations of oxygen; **Figure 12**; **Figure 13**), based on higher rates of oxygen-based respiration estimated during tidal isolation periods compared to rates estimated during tidal flushing periods. The higher rates of respiration may likely contribute to a higher frequency of nighttime hypoxia during periods of tidal isolation because of the depletion of oxygen in the pond water was not offset by inputs of water from surrounding creeks.

Tidal flushing plays an integral role in shaping the biogeochemistry, ecology, and geomorphology of salt marshes, and they play similar roles in the smaller scale of salt marsh ponds. The diurnal pattern in oxygen concentration change is affected by tidal flushing, and having established the conditions during isolated periods better allows for the investigation of tidal inundation. Nighttime tidal flushing, among others, causes replenishment in Pond 1 with inputs of oxygen (**Figure 18**), which created a nighttime peak in oxygen concentrations. This effect on oxygen concentration needs to be accounted for in metabolism calculations, something that has not been done yet (Spivak et al., 2017). During the three days of spring tides, the timing of the night time peaks occurs in a time that was usually excluded from estimation of respiration. Thus, for this time period, it was possible to estimate higher respiration rates for this time period than during tidal isolation when the system was hypoxic. Still, the rates are lower than our DIC based rates from Session 3. This suggests that the influx of oxygen via tidal flooding in our example is not sufficient to estimate the true rates of respiration.

As stated earlier, the rates of metabolism estimated using oxygen measurements underestimate the true rates of pond water metabolism. These estimates tend to miss some anaerobic processes (e.g., sulfate reduction). There is a possibility that the three nights in which I looked at the effect of tidal flushing are not the most optimal scenario, because of inundation of

the marsh platform during the daytime as well. Tidal flushing during the day results in a dilution effect of oxygen, as the saturated pond water essentially loses oxygen to surrounding creeks and streams as it becomes inundated. It would be more useful for my test when inundation actually occurs in the time frame I usually used for the calculations of respiration (i.e., 20:15 to 3:15 local time). The rates of metabolism may also miss some physical processes occurring in the pond (e.g., oxygen ebullition). The rates of calculations are based on the assumption of a diffusive flux, so if oxygen is transported by bubbles, we do not measure that. This may lead to an underestimation of GPP mostly. Consequently, my oxygen-based rates of respiration likely underestimate the true rate of respiration that actually occurs in the ponds. There also may have been errors in regards to our multi-parameter sensors (e.g., calibration error, probe sensitivity). Furthermore, the equations and parameters used to calculate my estimates of gas exchanges can be a source of uncertainty, as the model I used was developed for fluxes within lake systems. Gas exchange parameterizations are a large source of uncertainty in any of these calculations.

4.2 Ponds as Part of the Landscape

The lower rates of metabolism found in Pond 2 may be due to different vegetation cover, different pond sizes, or different sampling periods. We can allude that differences in plant communities of ponds may be the most likely driver contributing to the carbon balance (Spivak et al., 2017). These differences may have arisen from spatial factors and likely affect whether the pond is net autotrophic (where GPP is greater than R) or net heterotrophic (where GPP is less than R) [**Figure 22**]. The differences in pond plant communities may also contribute to the frequency in nightly hypoxic conditions. I found that Pond 1 contained an abundant population of *R. maritima* alongside other photosynthetic organisms, while Pond 2 contained macroalgae but not submerged vascular vegetation. Spivak et al., 2017 showed highest rates of metabolism

in Pond 1 compared to two other ponds. Pond 1 was also the only one of the intensively studied ponds that was autotrophic during the entire season. While the presence of *R. maritima* may certainly affect the balance between net autotrophic and net heterotrophic characteristics of the ponds.

Multiple factors seem to affect the differences in pond plant communities of Pond 1 and Pond 2. Further studies of pond plants are needed to understand these factors, with particular importance given to the dispersal of seeds and propagules. *R. maritima* cannot grow under low light conditions (Orth and Moore, 1988), so the differences in light conditions may be a factor in the variation in coverage across the ponds. Another influential factor in the differences in pond plant communities may be the incomplete tidal exchange and slow water velocities during periods of inundation (Spivak et al., 2017). Seeds from submerged grasses and spores of macroalgae settle out of surface waters rapidly, and distances of dispersal lie contingent on current velocities and organismal vectors (e.g., fish, waterbirds) [Agami and Waisel, 1988; Charalmanbidou et al., 2003; Gaylord et al., 2002; Orth et al., 1994]. The patterns of dispersal of *R. maritima* and macroalgae may be similar to those of the emergent grasses of the marsh platform. Seeds of these emergent grasses can be localized, and distribution of seeds is strongly corresponded to the patterns of adult plant abundance across the marsh platform (Rand, 2000).

Dispersal of *R. maritima* seeds and macroalgae propagules may be localized because of the ineffective transport of incoming tide water during inundation, yet it is unclear how the pond plant communities of Pond 1 starkly contrasts with those of Pond 2. It is critical to recognize the contributions of both dispersal mechanisms and succession processes to understand population dynamics of plants (Eriksson and Ehrlén, 1992, Menge and Sutherland, 1987, Schupp and Fuentes, 1995). The abundances and distribution of plant and algal populations across the two

ponds may also reflect an amalgam of abiotic factors (e.g., nutrient recycling, location of pond) rather than biotic factors such as top-down control from herbivores and competition from other species.

Higher plant abundance leads to not only to an influx of atmospheric CO₂, but also faster primary production rates, lower DIC concentrations, lower algal fractionation factors, and more frequent nighttime hypoxia (Spivak et al., 2018). The higher abundance of benthic macroalgae can also lead to high sediment DIC flux to surface waters, as well as faster sediment respiration rates. It is important to note that coverage of *R. maritima* in Pond 1 has decreased in past few years (from ~75% in 2014 to ~35% in 2017) [Spivak et al., 2017]. This suggests that the rates of metabolism in Pond 1 will likely change over time and vary with changes in abundances of primary producers and pond plant community composition. The composition of pond plant communities is an influential factor in the balance between pond autotrophy and pond heterotrophy, and continual decline in coverage of *R. maritima* may lead to an eventual shift to heterotrophy in Pond 1. This may be of particular concern, due to the relatively large size of Pond 1 in comparison to other ponds of the high marsh. If larger ponds such as Pond 1 shift to heterotrophy, we can expect more net CO₂ emission from the pond. I believe that the ability to predict future effects of ponds on the whole marsh ecosystem functionality lie contingent on a greater understanding of the relationship between pond plant communities and landscape heterogeneity. Furthermore, studies of controls on plant distributions are needed in order to make estimates of metabolism throughout the entire marsh landscape.

Often times the metabolism rates reported for salt marshes reflect only the contributions of emergent grasses and soils. Metabolism at the landscape scale is prone to overestimate both rates of NEP and R (Spivak et al., 2017). Contributions from ponds, however, are neglected. This

is because pond contributions to ecosystem metabolism remain unknown for the most part. Metabolism rates of salt marsh ponds that have varying levels of tidal flushing may be the missing pieces of information that could further develop an understanding of pond contributions. Further understanding of the roles of ponds in the whole landscape estimates of metabolism requires measurements of NEP and R in more ponds for longer periods. It is also important to have further studies that explore the potential variations of atmospheric and sediment gas exchange rates due to factors of primary producer communities, sediment composition, and pond water chemistry. Supplementary information regarding accurate estimates of anaerobic respiration, pond expansion, and tidal flushing export will also be beneficial.

As stated earlier, we have not yet developed a comprehensive understanding of pond biogeochemistry, which can be a determinant in potential future creation or expansion of ponds. An integral contributor to pond expansion and deepening was found to be sediment respiration based on sediment core data that are similar to data in this study (Spivak et al., 2018). There is still a large variability in ponds, including size and plant communities (Spivak et al., 2018), and all of these factors will be influential on the progression of pond expansion.

5. Summary

In summary, I found that salt marsh ponds are heterogeneous systems that can be influenced by many biotic and abiotic factors. Despite proximity and similar elevation, the two ponds differed in vegetation communities and size.

I found that tidal flushing plays an important role in replenishing oxygen during nighttime hypoxia and diluting oxygen during daytime productivity. Tidal flushing at night provided for an influx of oxygen into the pond, which consequently allowed for a better estimate

of oxygen-based rates of respiration. However, more data is needed to provide significant evidence that tidal flushing affects rates of metabolism in ponds. Overall, it was important to recognize the need for more than one metric for estimating rates of respiration. Using only oxygen concentrations tended to exclude anaerobic processes, and thus led to an underestimation of pond metabolism. Using DIC in conjunction with oxygen helped us to calculate a more representative estimate of metabolism.

Acknowledgements

Thanks to my advisor Tara Pisani Gareau for her comments for this paper, as well as her guidance and motivation to push me throughout my academic semesters. Special thanks to Inke Forbrich, for not only being my secondary advisor for this paper, but also being a wonderful supervisor during my time at MBL and a wise mentor for the past year. Thanks to Amanda Spivak and her team for their assistance during our 24-hour sampling session. Thanks to Anne Giblin for her incredible knowledge of the salt marsh ecosystem and its functionalities. I appreciate the support from the rest of MBL Ecosystems Center members, as well as the NSF-funded PIE-LTER for the opportunity to work in a marvelous environment. I appreciate the support from Boston College for giving me the opportunity to write and present my senior thesis.

References

- Adam, P. 1990. The saltmarsh biota. Saltmarsh Ecology. Cambridge University Press, New York, NY.
- Adamowicz, S. C., and Roman, C. T. 2005. New England salt marsh pools: A quantitative analysis of geomorphic and geographic features, *Wetlands*, 25(2), 279-288.
- Agami, M. and Waisel, Y. 1988. The role of fish in distribution and germination of seeds of the submerged macrophytes *Najas marina* L. and *Ruppia maritima* L. *Oecologia*, 76, 83-88.
- Ahearn, D. S., Viers, J.H., Mount, J. F., Dahlgren, R. A. 2006. Priming the productivity pump: Flood pulse driven trends in suspended algal biomass distribution across a restored floodplain, *Freshwater Biology*, 51(8), 1417-1433.
- Allen, JRL and Pye, K. 1992. Saltmarshes: morphodynamics, conservation, and engineering significance. Cambridge University Press. Cambridge, UK.
- Barbier, E. B., Hacker, S. D., Kennedy, C., Koch, E. W., Stier, A. C., Silliman, B. R. 2010. The value of estuarine and coastal ecosystem services, *Ecological Monographs*, 81(2), 169-193.
- Bertness, M. D. 1991. Interspecific Interactions among High Marsh Perennials in a New England Salt Marsh. *Ecological Society of America*, 72(1), 125-137.

- Bird, E. 2008. Coastal geomorphology: an introduction. John Wiley & Sons Ltd, West Sussex, England.
- Bromberg-Gedan, K., Silliman, B.R., and Bertness, M.D. 2009. Centuries of human driven change in salt marsh ecosystems, *Annual Review of Marine Science*, 1: 117-141
- Burdick, D. M., and Mendelsohn, I. A. 1990. Relationship Between Anatomical and Metabolic Responses to Soil Waterlogging in the Coastal Grass *Spartina patens*, *Journal of Experimental Botany*, 41(2), 223-228.
- Chapman, V.J. 1974. Salt marshes and salt deserts of the world. Phyllis Claire Chapman, Germany.
- Charalambidou, I., Santamaria, L., and Langevoord, O. 2003. Effect of ingestion by five avian dispersers on the retention time, retrieval and germination of *Ruppia maritima* seeds. *Functional Ecology*, 17(6), 747-753.
- Eriksson, O., and Ehrlén, J. 1992. Seed and microsite limitation of recruitment in plant populations. *Oecologia*. 91, 360-364.
- Forbrich, I., and Giblin, A. E. 2015. Marsh-atmosphere CO₂ exchange in a New England salt marsh, *Journal of Geophysical Research: Biogeosciences*, 120(9), 1825-1838.

- Ganju, N. K., Kirwan, M. L., Dickhudt, P. J., Guntenspergen, G. R., Cahoon, D. R., and Kroger, K. D. 20015. Sediment transport-based metrics of wetland stability, *Geophysical Research Letters*, 42(19), 7992-8000.
- Gaylord, B., Reed, D. C., Raimondi, P. T., Washburn, L., and McLean, S. R. 2002. A physically based model of macroalgal spore dispersal in the wave and current-dominated nearshore, *Ecology*, 83(5), 1239-1251.
- Greenway, H., Armstrong, W., Colmer, T. D. 2006. Conditions Leading to High CO₂ (>5 kPa) in Waterlogged – Flooded Soils and Possible Effects on Root Growth and Metabolism. *Annals of Botany*, 98(1), 9-32.
- Hopkinson, C. S., Cai, W. J., and Hu, X. 2012. Carbon sequestration in wetland dominated coastal systems – a global sink of rapidly diminishing magnitude. *Current Opinion in Environmental Sustainability*. 4(2), 186-194.
- Johnston, M. E., Cavatorta, J. R., Hopkinson, C. S., Valentine, V. 2003. Importance of metabolism in the development of salt marsh ponds, *Biological Bulletin*, 205, 248-249.
- Kearns, P. J., Holloway, D., Angell, J. H., Feinman, S. G., and Bowen, J. L. Effect of short-term, diel changes in environmental conditions on active microbial communities in a salt marsh pond. *Aquatic Microbial Ecology*, 80, 29-41.

- Mariotti, G., and Fagherazzi, S. 2013. Critical width of tidal flats triggers marsh collapse in the absence of sea-level rise, *Proceedings of the National Academy of Sciences of the United States of America*, 110(14), 5353-5356.
- McLeod, E., Chmura, G. L., Boullon, S., Salm, R., Björk, M., Duarte, C. M., Lovelock, C. E., Schlesinger, W. H., and Silliman, B. R. 2011. A blueprint for blue carbon: Toward an improved understanding of the role of vegetated coastal habitats in sequestering CO₂, *Frontiers in Ecology and the Environment*, 9(10), 552-560.
- Mcowen, C., Weatherdon, L., Bochove, J. W., Sullivan, E., Bluth, S., Zockler, C., Stanwell Smith, D., Kingston, N., Martin, C. 2017. A global map of saltmarshes. *Biodiversity Data Journal*. 5.
- Melzner, F., Thomsen, J., Koeve, W., Oschlies, A., Gutowska, M. A., Bange, H. W., Hansen, H. P., Kortzinger, A. 2012. Future ocean acidification will be amplified by hypoxia in coastal habitats, *Marine Biology*, 160, 1875-1888.
- Mendelssohn, I. A., and McKee, K. L. 1988. *Spartina Alterniflora* die-back in Louisiana: Time course investigation of soil waterlogging effects, *Journal of Ecology*, 76(2), 509-521.

- Menge, B. A., and Sutherland, J.P. 1987. Community regulation: variation in disturbance, competition, and predation in relation to environmental stress and recruitment. *American Naturalist*, 130, 730-757.
- Milette, T. L., Argow, B. A., Marcano, E., Hayward, C., Hopkinson, C. S., and Valentine, V. 2010. Salt Marsh Geomorphological Analyses via Integration of Multitemporal Multispectral Remote Sensing with LIDAR and GIS, *Journal of Coastal Research*, 809-816.
- Miller, W. R., and Egler, F. E., 1950. Vegetation of the Wequetequock-Pawcatuck tidal-marshes, Connecticut, *Ecological Monographs*, 20(2), 143-172.
- Nixon, S. W. 1982. The ecology of New England high salt marshes: A community profile. United States Department of the Interior, Washington, D.C., U.S.A.
- Orth, R. J., Luckenbach, M., and Moore, K. A. 1994. Seed dispersal in a marine macrophyte: Implications for colonization and restoration, *Ecology*, 75(7), 1927-1939.
- Orth, R. J. and Moore, K. A. 1988. Distribution of *Zostera marina* and *Ruppia maritima* sensu lato along depth gradients in the lower Chesapeake Bay, U.S.A. *Aquatic Botany*, 32(3), 291-305.

Pethick, J. 1984. An introduction to coastal geomorphology. Edward Arnold, London.

Rand, T. A. 2000. Seed dispersal, habitat sustainability and the distribution of halophytes across a salt marsh tidal gradient, *Journal of Ecology*, 88(4), 608-621.

Salt Marshes. (n.d.). from

<http://www.oceanhealthindex.org/methodology/components/salt-marsh-area>

Schepers, L., Kirwan, M., Guntenspergen, G., and Temmerman, S. 2017. Spatio-temporal development of vegetation die-off in a submerging coastal marsh, *Limnology and Oceanography*, 62(1), 137-150.

Schupp, E.W., and Fuentes, M. 1995. Spatial patterns of seed dispersal and the unification of plant population ecology. *Ecoscience*, 2, 267-275.

Spivak, A. C., Gosselin, K. M., Howard, E., Mariotti, G., Forbrich, I., Stanley, R., and Sylva S.P. 2017. Shallow ponds are heterogeneous habitats within a temperate salt marsh ecosystem. *Journal of Geophysical Research: Biogeosciences*, 122, 1371-1384.

Spivak, A. C., Gosselin, K. M., Sylva, S. P. 2018. Shallow ponds are biogeochemically distinct habitats in salt marsh ecosystems. *Limnology and Oceanography*.

Staehr, P. A., Bade, D., Van de Bogert, M. C., Koch, G. R., Williamson, C., Hanson, P., Cole, J.

J., and Kratz, T. 2010. Lake metabolism and the diel oxygen technique: State of the science. *Limnology and Oceanography: Methods*, 8(11).

Timmerman, C. M., and Chapman, L. J. 2004. Patterns of Hypoxia in a Coastal Salt Marsh:

Implications for Ecophysiology of Resident Fishes. *Florida Scientist*, 67(1), 80-91.

Tolley, P. M., and Christian, R. R. 1999. Effects of Increased Inundation and Wrack Deposition

on a High Salt Marsh Plant Community. *Estuaries*, 22(4), 944-954.

Vachon, D., and Prairie, Y. T. 2013. The ecosystem size and shape dependence of gas transfer

velocity versus wind speed relationships in lakes, *Canadian Journal of fisheries and Aquatic Sciences*, 70(12), 1757-1764.

van Huissteden, J., and van de Plassche, O. 1998. Sulphate reduction as a geomorphological

agent in tidal marshes ('Great Marshes' at Barnstable, Cape cod, USA), *Earth Surface Processes and Landforms*, 23(3), 223-236.

Wannikhof, R. 2014. Relationship between wind speed and gas exchange over the ocean

revisited, *Limnology and Oceanography: Methods*, 12(6), 351-362.

Wilson, C. A., Hughes, Z. J., FitzGerald, D. M., Hopkinson, C. S., Valentine, V., and Kolker, A.

S. 2014. Saltmarsh pool and tidal creek morphodynamics: Dynamic equilibrium of northern latitude saltmarshes?, *Geomorphology*, 213, 99-115.

Winslow, L. A., Zwart, J. A., Batt, R. D., Dugan, H. A., Wollway, R. L., Corman, J. R., Hanson,

P. C., and Read, J. S. 2016. LakeMetabolizer: An R package for estimating lake metabolism from free-water oxygen using diverse statistical models, *Inland Waters*, 6(4). 622-636.

Woodroffe, CD. 2002. Coasts: form, process and evolution. Cambridge University Press. New York, NY.